Computational Fluid Dynamics of a Wind Turbine

A Major Qualifying Project

Submitted to the faculty of

Worcester Polytechnic Institute

In partial fulfillment of the requirements for the

Degree of Bachelor of Science

Submitted by:

_____   _____

Harrison He (ME)   Alan Hunt (ME)

_____   _____

Charlotte Moore (ME)   Theodore Wallach (ME)

Approved By:

_____   _____

Professor David Planchard   Professor John Hall

Advisor (ME)   Advisor (ME)

Date: April 23, 2018

Contents

Figures

Tables

Equations

Abstract

Currently, it is difficult to determine wind speed or power output for a proposed wind turbine without on-site wind speed data and computational fluid dynamics (CFD) analysis software. Our Major Qualifying Project is to analyze the results from SolidWorks's Flow Simulation package and the data that was collected from a custom designed and manufactured wind turbine test rig. To do this, air was rotated through modeled wind turbine blades in the CFD simulations. We found there is a constant ratio between the slopes of the free-spinning and max power RPM trend lines of the blades. On-site, an anemometer collected local wind speeds while a free spinning wind turbine test rig measured the RPM. We found that a lighter wind turbine is more efficient because of a faster spool up time.

Acknowledgments

We would like to thank our advisors, Professors David Planchard and John Hall, for their continuous support and guidance. We would also like to thank Joe Galliera from D'Assault Systèmes for his in-depth expertise in SolidWorks Flow Simulation. In addition, we would like to thank Keshuai "Cosine" Xu for his help in software coding. Finally, we would like to thank Laura Robinson, the librarian for project-based learning and research impact, for her help on references.

1.0 Introduction

Renewable energy is being sought out as nonrenewable energy sources continue to become scarce and hazardous to the Earth. Two common forms of renewable energy are solar energy and wind energy. Solar power exists on both an industrial scale and residential scale. However, wind energy is almost exclusively available on the industrial scale. With solar power, it is easy to predict power output given the angle of the solar panels and location of installation without any on-site testing. With wind power, it is much more complicated given the unpredictable nature of wind. Furthermore, two nearby locations could have vastly different wind characteristics but would have almost identical solar properties. In order to bring wind energy on the same level of accessibility as solar power, it is necessary to calculate its potential power output. This Major Qualifying Project (MQP) aims to provide data collection through software means for predictions of residential wind turbine power outputs.

2.0 Background

In order to fully understand the usage of CFD in wind turbine applications, it is necessary to go over a few key concepts: wind turbines and power generated from the wind.

2.1 Wind Power

Power, in general, is the transfer of energy over time. In a rotational setting, power is denoted as:

$$P = T\omega \tag{1}$$

Where P is power, T is torque, and ω is angular speed. For a wind turbine, the power in the wind can be further shown as:

$$P_w = \frac{1}{2}\rho A v^3 \tag{2}$$

Where P_w is the power in the wind, ρ is the density of air, A is the reference cross-sectional area that the wind turbine blades sweep through, and v is the wind speed. For a typical wind turbine installed at a location where the temperature is 15 °C and the pressure is 1 atmosphere, the density of air is 1.225 $\frac{kg}{m^3}$. The power of the wind is proportional both to the square of the diameter of the wind turbine blades and the cube of the wind speed. Because of this, we will need to use some method other than finding the average wind speed to determine the total power in the wind. A better approach is to find the average cube of wind speed (as opposed to the cube of average wind speed). For example, given a temperature of 15 °C, a pressure of 1 atm, and 1 m² of cross-sectional area, the energy contained in 100 hours of 6 m/s winds is 13,230 Watt-hours. On the other hand, the sum of the energy contained in 50 hours of 3 m/s winds and 50 hours of 9

m/s winds is 23,153 Watt-hours. Even though the number of hours and average wind speed were the same, the two scenarios produced vastly different energy outputs [1].

Wind speeds can vary in a given location, so it is necessary to account for the probability that a certain wind speed will occur. This is generally done by recording wind data for a certain amount of time and dividing the amount of time a wind speed occurs by the total time recorded, as seen below:

$$Probability\ (v = v_i) = \frac{Number\ of\ hours\ v_i\ occured}{Total\ number\ of\ hours} \tag{3}$$

And so, the true, weighted average of wind speed is as follows:

$$v_{avg} = \sum_i [v_i * Probability\ (v = v_i)] \tag{4}$$

Therefore, the average cube of wind speed is simply:

$$(v^3)_{avg} = \sum_i [v_i^3 * Probability\ (v = v_i)] \tag{5}$$

The average cube of the wind speed is much different than simply cubing the average wind speed. The wind speed is measured with anemometers, which spin at a rate proportional to the wind speed [1].

There is a maximum efficiency, known as the Betz limit, associated with the power that can be extracted from a wind turbine. This limit of efficiency exists because there would have to be absolutely no kinetic energy exiting the wind turbine for the wind turbine to extract all the upwind kinetic energy that goes into it. Because there is always wind blowing past the wind turbine (at a velocity that is smaller than the upwind speed), there must be some energy lost. The

Betz limit occurs when the downwind velocity slows down to one-third of the upwind velocity, in which the wind turbine can extract $\frac{16}{27}$ (59.26%) of the theoretical power in the wind. By the laws of physics, no wind turbine is capable of extracting any energy that exceeds the Betz limit. The best modern wind turbines can obtain 80% of this efficiency, in which the turbine blades spin neither too slow nor too fast and have optimized geometry [1].

Other factors that can affect wind turbine power are altitude and temperature. These are related to air density by the ideal gas law, which is proportional to the power of the wind. Wind speeds closer to the ground are affected by friction incurred from contact with the Earth's surface as well as trees and buildings. Because wind turbine power is proportional to the cube of wind speed, creating higher towers for a wind turbine can increase generated power [1].

2.2 Wind Turbines

There are two classifications of wind turbines: the horizontal axis wind turbine (HAWT) and the vertical axis wind turbine (VAWT). Most large-scale wind turbines are HAWTs, in which the blades are rotating about a horizontal axis. HAWTs can be further classified into upwind and downwind turbines. The wind blows into the front side of the blades of upwind HAWTs and the wind blows into the back side of the blades of downwind HAWTs. Despite being able to naturally orient themselves in the direction of the wind, downwind turbines are plagued by the issue that when the blades are behind the tower, there is reduced wind, leading to potential blade failure and decreased power output. Upwind HAWTs, on the other hand, require more complex control systems to make the blades face the wind. This results in increased power output and reduces the chances of blade failure [1].

Even though HAWTs have certain characteristics that make them harder to use and maintain, VAWTs are primarily disadvantaged because their blades operate closer to the ground. Because of this, they experience lower wind speeds and thus have lower power outputs. VAWTs do have a few advantages, such as the fact that their generators and gearboxes can be easily serviced because they are on the ground. In addition, they also do not need a control system because they do not need to orient with the wind direction [1].

In general, an increase in the number of blades decreases the efficiency of blades themselves, so it is better to have fewer blades. Despite this, three blades are preferable to two blades because they have a smoother operation, even if two blades can generate more power because they spin at a faster rate [1].

Regardless of classification, there are various characteristics that are important to all wind turbines. First and foremost, the power output of a wind turbine is oftentimes the main motivation for both its production and its purchase. Wind turbines that are sold usually come with a graph that relates wind speed to power. There are some important wind speeds that determine this power output. Namely, the cut in wind speed is the minimum wind speed needed to overcome friction and generate power. In addition, the rated wind speed is the maximum wind speed that the wind turbine is designed to handle so that the generator is not damaged. There is also the cut out wind speed which is the wind speed in which the wind turbine must be shut down to prevent excessive damage to the generator. These wind speeds are crucial to know when testing and designing a wind turbine [1].

3.0 Preliminary Work

As part of the MQP, we wished to analyze wind data in both in a simulation and in a real-life setting. To do this we thought it would be best to use a computational fluid dynamics (CFD) software, SolidWorks Flow Simulation, and to construct a wind turbine test rig by manufacturing and purchasing the various individual components and assembling them in a fashion that would suit our needs.

3.1 Computer Aided Design Models

In order to find simulated power output of the wind turbine test rig, a Computer-Aided Design (CAD) model of the wind turbine test rig blades was needed. As such, the blades were modeled in SolidWorks, a CAD software, as seen in Figure 1:
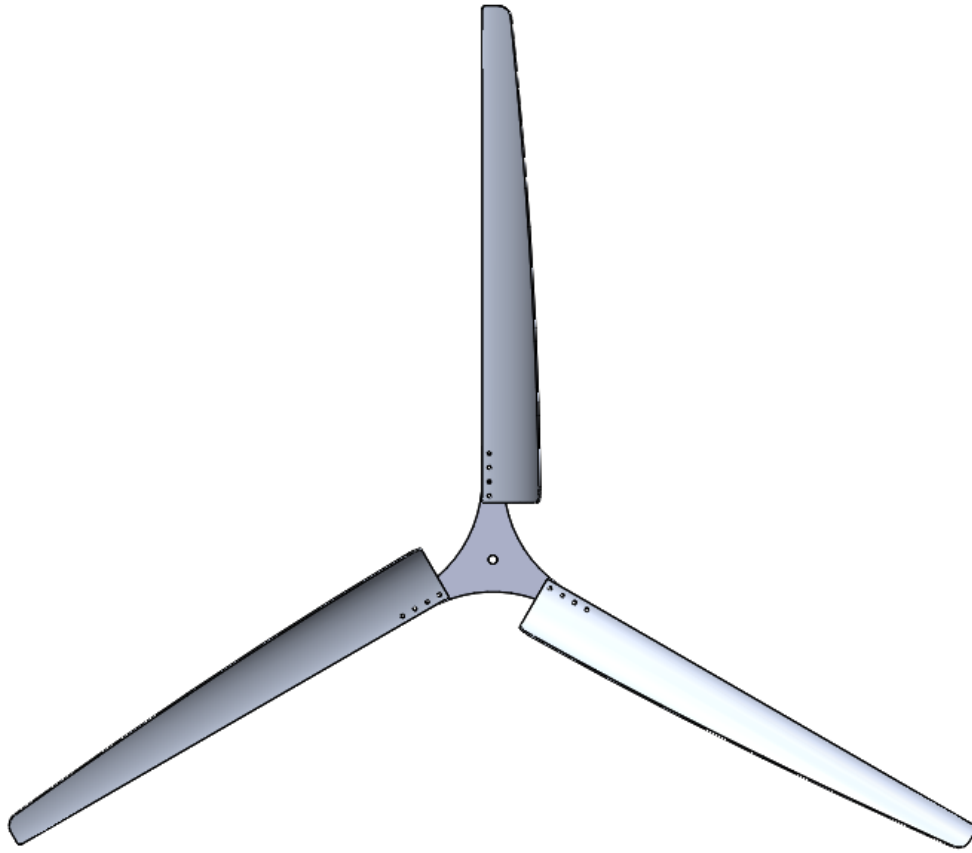
Figure 1 - Computer Aided Design Model of Wind Turbine Test Rig Blades

The blades were modeled by first modeling a tube and creating a plane tangent to the surface area of the tube to perform a sketch. The material that was not needed was cut away, similar to how a sculpture is conceived, and the remaining material was a singular turbine test rig blade that wrapped around the tube's surface area. Various aspects of the fan blade were measured and inputted into SolidWorks so that the model could match the physical wind turbine test rig. After that, the fillets were inserted and holes were made for the bolts to fit in.

Using SolidWorks, we decided to model only a third of the wind turbine test rig blade hub because there are three symmetric blades. Within this third, all of the linear lengths were measured so that the rest of the part dimensions could be determined. Afterward, the fillets and

holes were added. This third was then rotated and copied twice to create the entire central part and the turbine test rig blades were assembled by putting together three blades and the central part.

3.2 Slip Ring Consideration

Slip rings are needed to transmit voltage and current across a rotating joint. Another option is to mount the generator vertically, connecting it to the wind turbine through a set of bevel gears. This allows the wind turbine to rotate about the generator. For the wind turbine test rig, we needed slip rings or a set of bevel gears since the nacelle must rotate but the pole underneath it remains stationary. We pursued the slip ring option over the bevel gear set because they are relatively inexpensive. The bevel gear set would be difficult to properly configure due to how they would inadvertently rotate the entire assembly because of transmission torque. Slip rings were needed because sensors were added to the wind turbine test rig. In a real-world case, slip rings would still be needed since either electrical power would be generated or sensors would be needed to calculate speed. There are two types of slip rings: pancake and drum. The pancake slip ring is a horizontal slip ring, as seen in Figure 2:
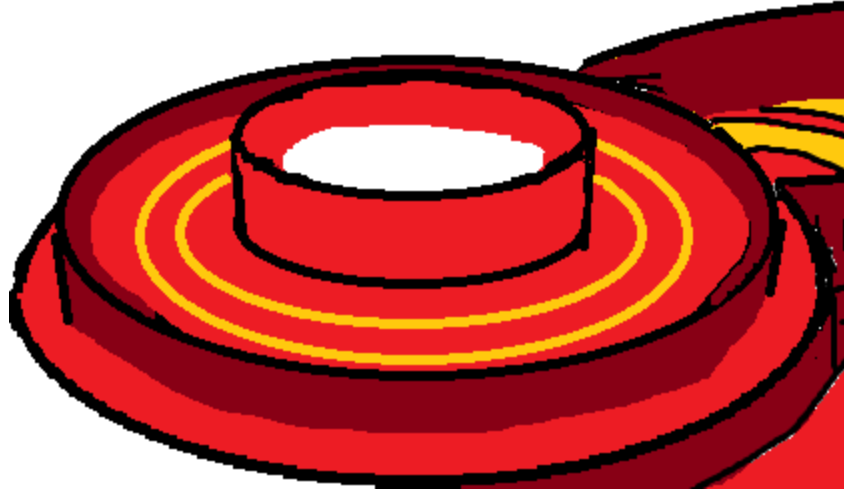
Figure 2 - Pancake Slip Ring [2]

Figure 3 shows a close-up of a pancake slip ring:
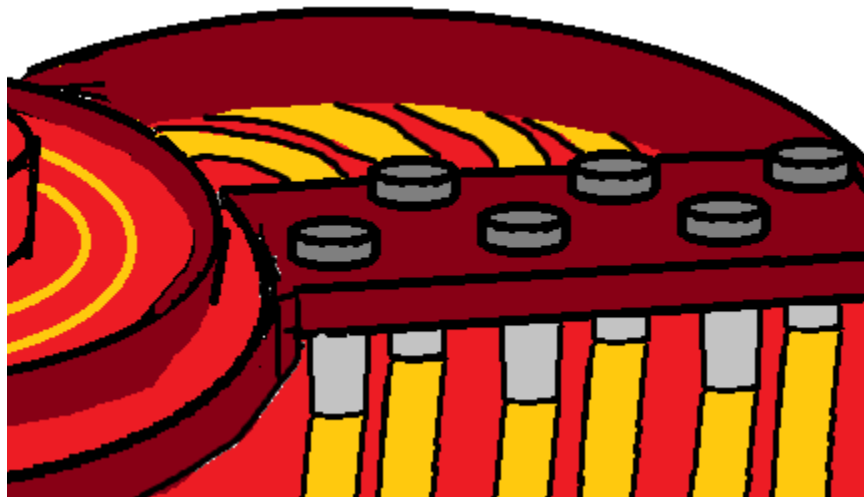
Figure 3 – Close-up of Pancake Slip Ring [2]

A drum slip ring is a vertical slip ring, as seen in Figure 4:
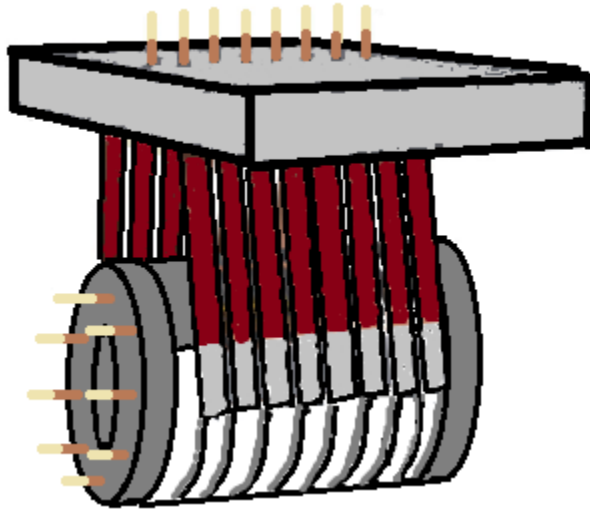
Figure 4 - Drum Slip Ring [3]

3.3 Pole mount

We created a model of the pole mount in SolidWorks, as seen below in Figure 5:
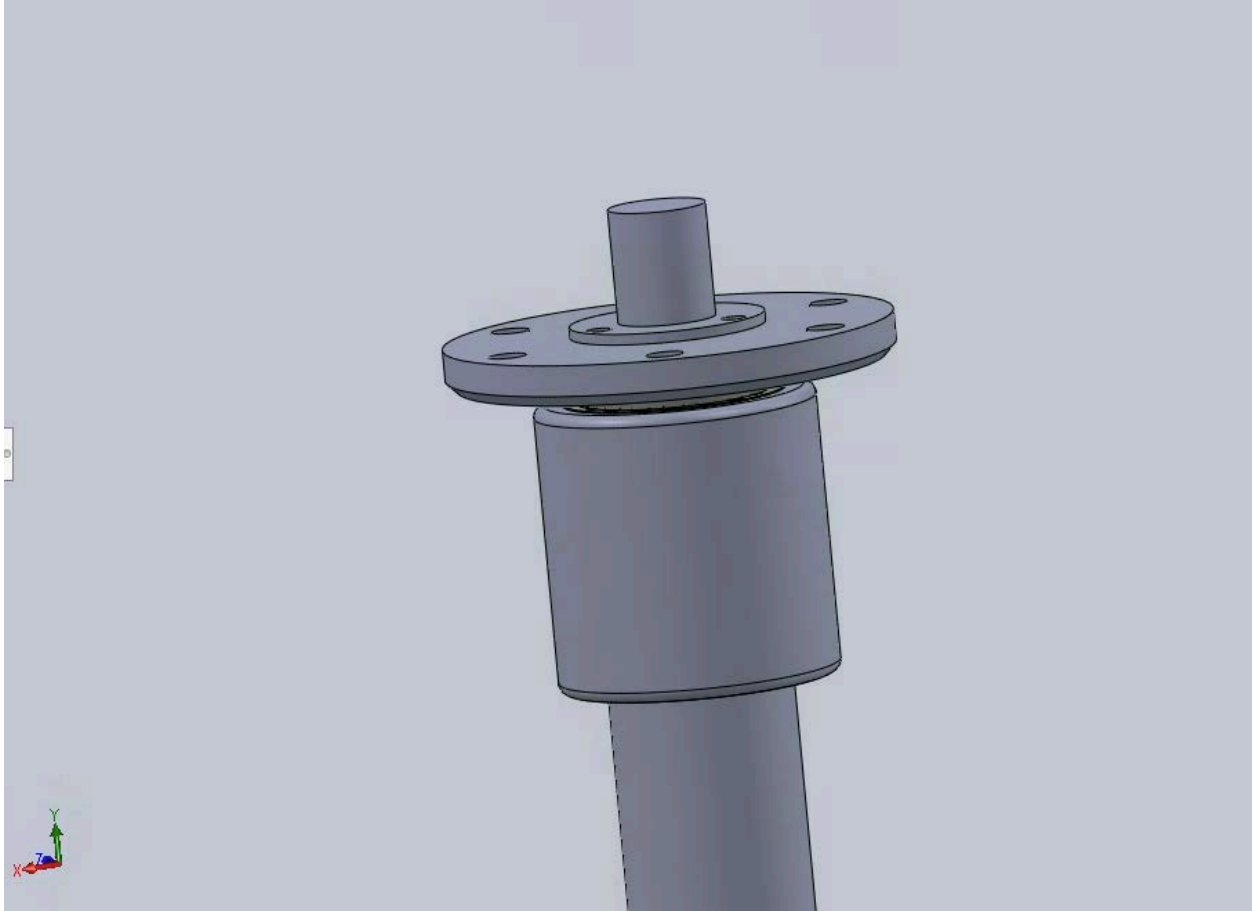
Figure 5 - Assembly of Pole Mount CAD Model

This assembly is made up of the pole and five other components. The bottom-most component is a 17-foot pole. There is an adapter shaft that mounts to the pole and contains two press-fit bearings within it. One of those is a tapered-roller bearing, as seen in Figure 6:

Figure 6 – Adapter Shaft

The pole mount was manufactured using a four-step process. The first two steps involved turning all of the features on the Haas ST-30 lathe. Starting with a solid round bar of aluminum, the top features were turned. The only external feature was a radius put on the face to eliminate the sharp corner. The center was drilled, and a boring bar was subsequently used to create the bore for the wires to go through, as well as the pocket for the tapered bearing to be pressed in.

The initial cut was intentionally made too small, so that the pocket could be measured, adjusted, and cut again to make a perfect press fit.

The second operation involved flipping the part around in the three-jaw chuck and cutting the features on the bottom of the part. Since the jaws on the lathe were not properly concentric for the first operation, the part was marked with a Sharpie marker indicating which jaw it was lined up with, then flipped around, and lined up with the same jaw. This ensured that the top and bottom bearings would be properly aligned. The face radius was added, and the bottom bearing press bore was included. Finally, a bore was added so that the threads could be included later.

The third step involved cutting the threads with a 1-1/4" NPT tap so that it could be threaded onto the pipe. This was done manually with a large tap handle, and the threads were cut most of the way into the bore.

The fourth step involved pressing the bearings into their respective bores. This was done using an arbor press. Care was taken to make sure the bearings were properly aligned and seated in the bore before being pressed in.

3.4 Base Plate

This base plate, as seen in Figure 7, was done in several operations, all using the Haas VM2 milling center.
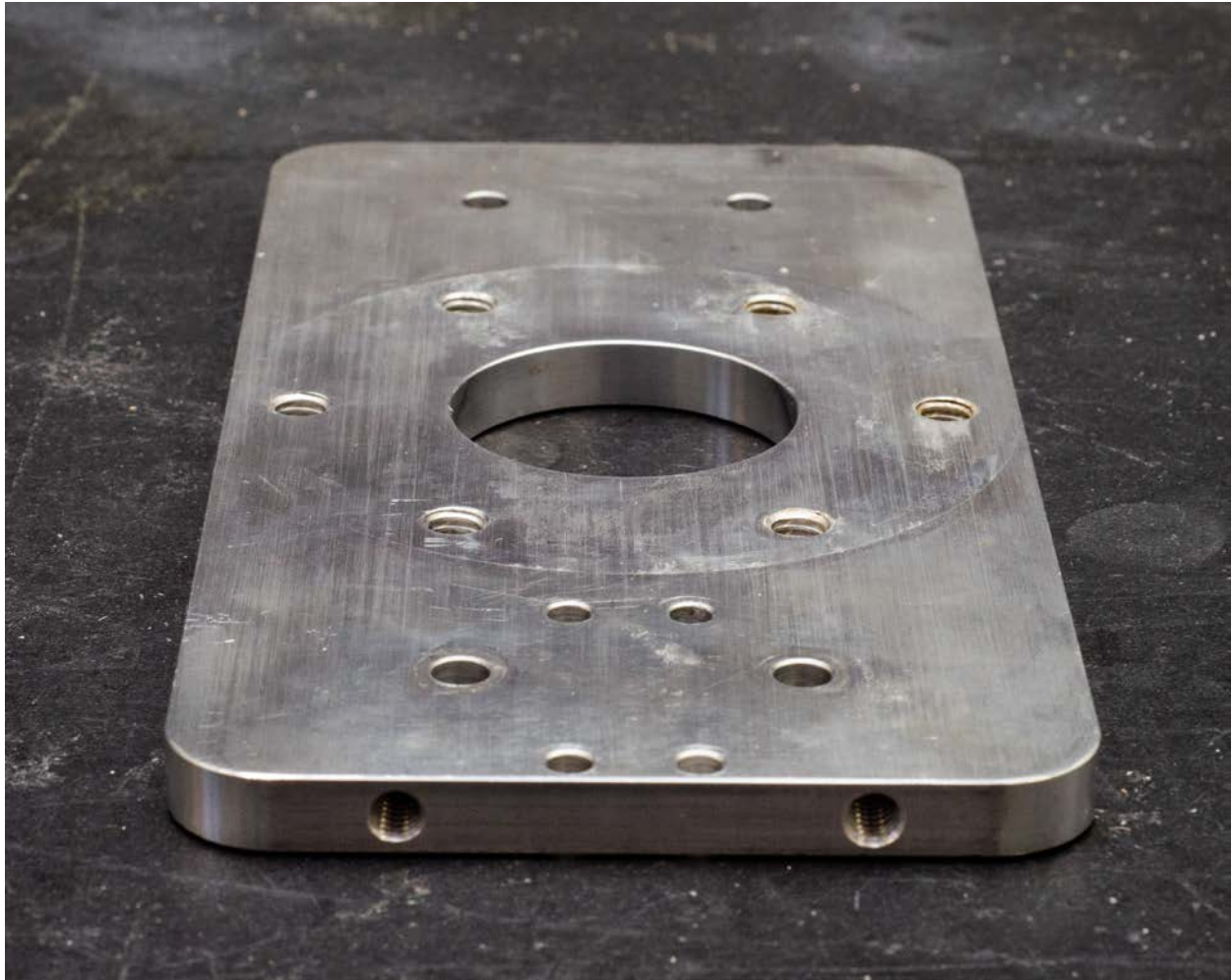
Figure 7 - Base Plate

The plate was cut to the rough shape on a bandsaw, then put into the VM2. The four edges of the part were squared up using a face mill, and the corners were rounded using an endmill. Once that was done, the features on the face of the part were done. The holes were all drilled, and the center bore was milled. Then, the part was taken out of the machine, and all of the holes that needed threads were hand tapped. The part was shelved for a while until the plastic

enclosure was made. Once the locations of the holes for the plastic enclosure had been determined, the part was put back into a MiniMill and holes were drilled on all four sides. The holes were tapped so that screws could be added to hold the enclosure on.

3.5 Slip Shaft

The slip shaft, as seen in Figure 8, attaches to the base plate and holds the slip ring.

Figure 8 - Slip Shaft

24

The slip rings attach to the slip shaft as seen in the assembly in Figure 5. This part was done in two major steps. The first step was done by putting a large round piece of aluminum stock into the ST-30 and turning the bottom features first. The smaller end of the part faced outwards to make manufacturing as easy as possible. The features were all turned, and the center hole was drilled. Then, the part was separated from the remaining stock using a vertical bandsaw. The part was then fixtured vertically in a MiniMill, and then the six mounting holes were drilled, and the center bore milled.

3.6 Bearing Mounts/Uprights

The bearing mounts and uprights, as seen in Figure 9, were manufactured in three steps.
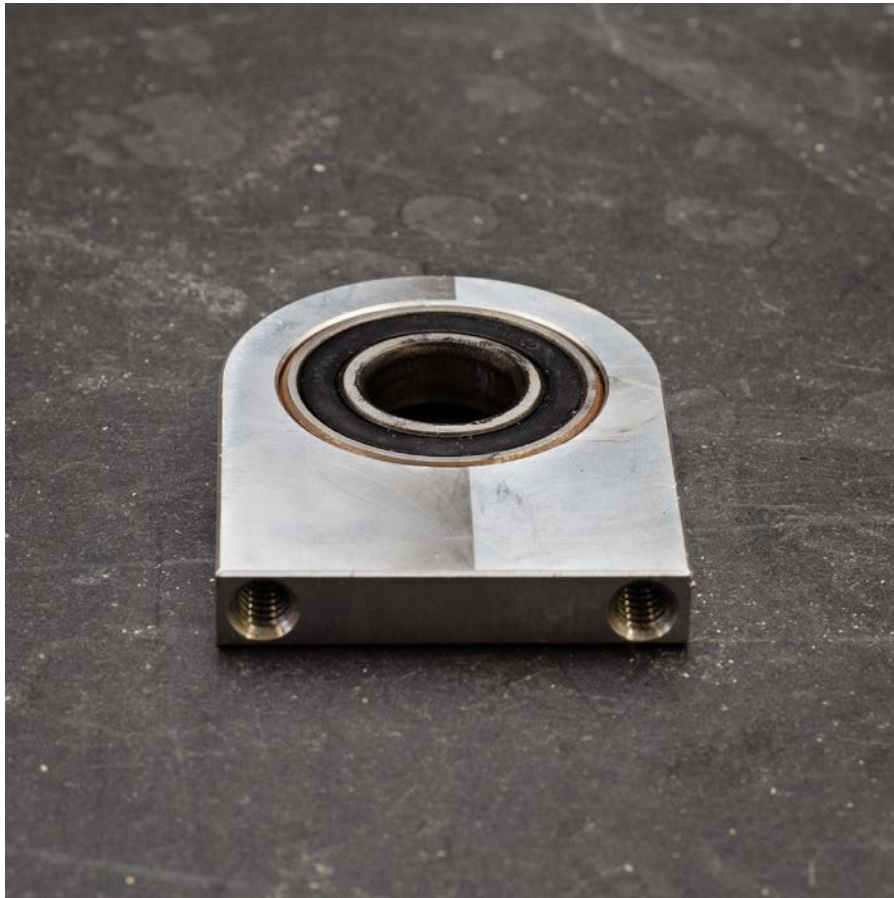
Figure 9 - Bearing Mount

First, the major profile was milled in the VM2 from a block of aluminum. This includes the outer profile, as well as the bearing press fit bore. The bore was intentionally made small first, then brought to size little by little so the bearing would press in perfectly. Once those features were done, the part was flipped over, and the remaining material was faced off to bring the part to size. Finally, the part was flipped with the bottom face facing upwards, so that the screw holes could be drilled. The screw holes were then hand tapped, and the bearings were put in. Unfortunately, the fit was loose, so the bearings would not press and stay in the holes. We used threadlocker to hold bearings in place to keep them from sliding out, thus preventing the need to manufacture two new parts.

3.7 Shaft

The shaft was manufactured from a round bar of stainless steel, as seen in Figure 10:

Figure 10 - Shaft

This was done using a two-step process in the Haas ST-10 lathe. Because the part was long, the part needed to be fixtured on one end using the collet on the spindle, and the other end needed to be stabilized by the tailstock. This ensured accurate and chatter-free machining. The first side was turned and then tested with the bearing. The bearing did not fit at first, so the shaft was turned down little by little until it fit. Then, the shaft was flipped around, so the other side could be turned, and the same process was used to make sure the other bearing would fit. Finally, a flat was ground onto the end of the shaft that would accept the shaft collar, so that the set screw would have a flat surface to rest up against.

3.8 Shaft Collar

The shaft collar is the part that connects the shaft to the plate that the three blades are connected to, as seen in Figure 11:

Figure 11 - Shaft Collar

This was done by milling a block of aluminum to the overall cylindrical profile, then flipping it over and removing the excess material. The three holes were drilled and tapped, then a set screw hole was added. The center bore was milled undersize, then steadily brought up in size until it slipped onto the shaft with a fairly tight fit.

3.9 Enclosure

The round opaque white part of the enclosure was cut to shape on the shear. Then, the holes were precisely drilled to line up with the screw holes on the base plate. The plastic was bent, and the screws installed to form the majority of the enclosure. Then, the two end pieces were cut out of clear acrylic on the laser cutter. After full assembly of the turbine, the pieces were all sealed with hot glue.

3.10 Synthesis of Wind Turbine Test Rig

In order to put everything together, there were electronics that needed to be used for the wind turbine. These electronics include the Hall Effect sensor and the ESP8266 which connects to Wi-Fi. In addition, there needed to be components (such as the bearings) that would hold the wind turbine shaft as well as the threaded rod for the tail of the wind turbine test rig. We also designed the base plate, which holds essentially everything, for the pole mount. The CAD model of the wind turbine test rig can be seen in Figure 12, Figure 13, Figure 14, Figure 15, and Figure 16:

Figure 12 - CAD model (Back Side)

Figure 13 - CAD Model (Front Side)
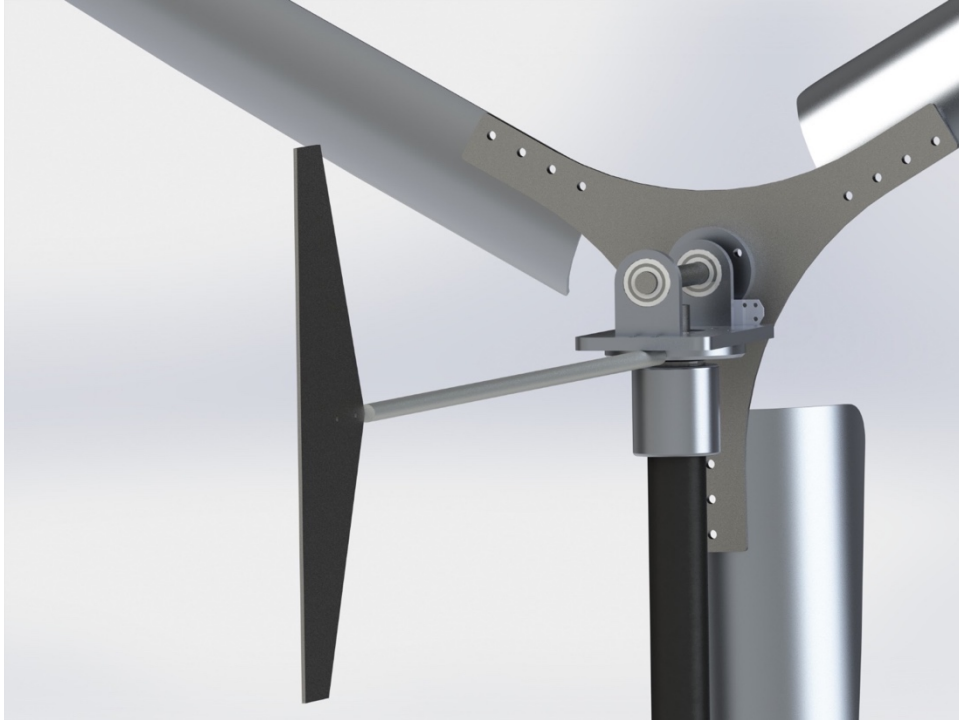
Figure 14 - CAD Model (Backside close up)
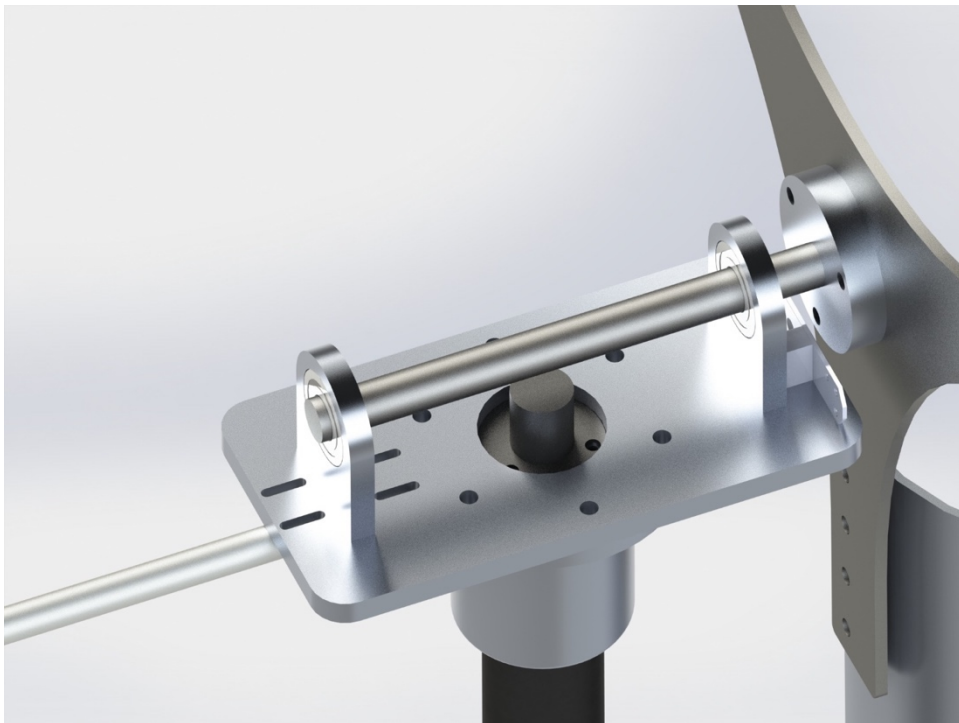
Figure 15 - CAD Model (Nacelle)

Figure 16 - CAD Model (Upward View)

The pole mount, as seen in Figure 17, has a pocket for the bearing to press into. A tapered roller bearing, as seen in Figure 18, has been pressed on to the top and the smaller bearing, as seen in Figure 19, has been put on the bottom. The slip ring connects to the slip shaft, as seen in Figure 20.

Figure 17 - Pole Mount

Figure 18 - Tapered Roller Bearing

Figure 19 - Smaller Bearing
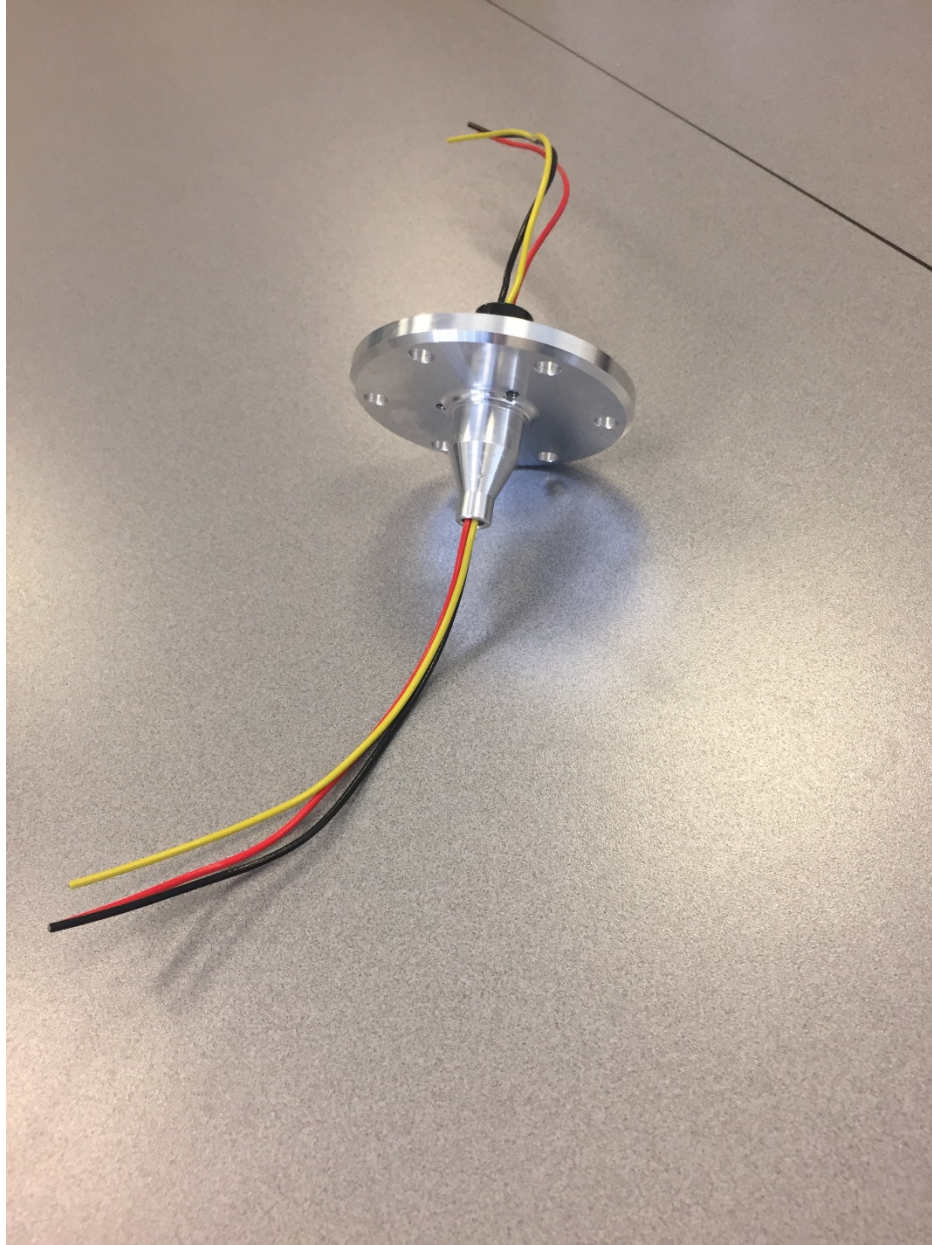
Figure 20 - Slip Ring with Slip shaft

3.11 Preparations for Installation

It was important to be aware that the ground would possibly freeze depending on the time of year. As such, we made the necessary preparations to install the wind turbine test rig into the ground. First and foremost, a sleeve was inserted two feet into the ground for the pole. In

addition, three stakes were hammered three feet into the ground for the guy wires. Finally, all of

the lengths of the guy wires were measured for future purposes. Figure 21 and Figure 22 show

the sleeve in the ground.

Figure 21 - Sleeve in the ground (1)

Figure 22 - Sleeve in the ground (2)

Other considerations for the installation include the fact that the wind turbine test rig was established with a 17-foot pole. This pole consisted of two poles joined together. Due to this, we did not wish it to take axial loading. This could be caused by wind if there are guy wires attached to it in certain areas. Therefore, we determined that it would be best to attach the guy wires as far up the pole as possible.

4.0 CFD Flow Simulation

A goal of this MQP is to analyze rotational flow simulations in SolidWorks. We hope that in the future this will allow companies and organizations to predict maximum potential wind turbine power output at specific residences. They would not be able to fully take financial advantage of their wind turbines if they did not know their maximum power outputs. In addition, preliminary background research pointed out the fact that the maximum power output is not only dependent on the machine but also the probability of wind speeds. As a result, it is necessary to optimize the wind turbine such that it will produce the most amount of power that takes both the wind turbine blades' rotational speed and the fastest wind speed of high probability while also factoring in the Betz limit.

Though ANSYS is a popular option for computational fluid dynamics and related applications, familiarity with SolidWorks ultimately led to it being the software of choice. SolidWorks, a computer-aided design software typically used for building models of machine designs, has a Flow Simulation package that can be used to determine the torque value that we desire.

4.1 Flow Simulation Setup

After some initial research and failed attempts to set up the flow simulation ourselves, we were put in contact with Joe Galliera who is the Senior Technical Sales Specialist for SolidWorks Simulation for D'Assasult Systèmes.

To begin a flow simulation, the Wizard button was clicked in the 2017-2018 SP 4.0 Academic SolidWorks Flow Simulation software to set up the Flow Simulation. From the pop-up window, units for velocity and pressure were changed to MPH and $\frac{lb_f}{in^2}$ respectively [4]. The Flow

Simulation was configured such that it would be an internal flow. It is not an external flow because of the volume control and how we created a boundary separating the flow from the rest of the environment [5]. In addition, the physical features were designated to be Rotation, with a Local (averaging) region type because the wind was only expected to travel in a single direction. Reference axis was set to Z given the orientation of the CAD model. Default fluid was set to air. For the initial conditions, velocity in the Z direction can be set to the linear wind speed required for each test. On the left sidebar under Rotating Region, Insert Rotating Region was clicked. Rotating region in the Computer-aided Design (CAD) model was selected, as seen in Figure 23:

Figure 23 - Rotating Region

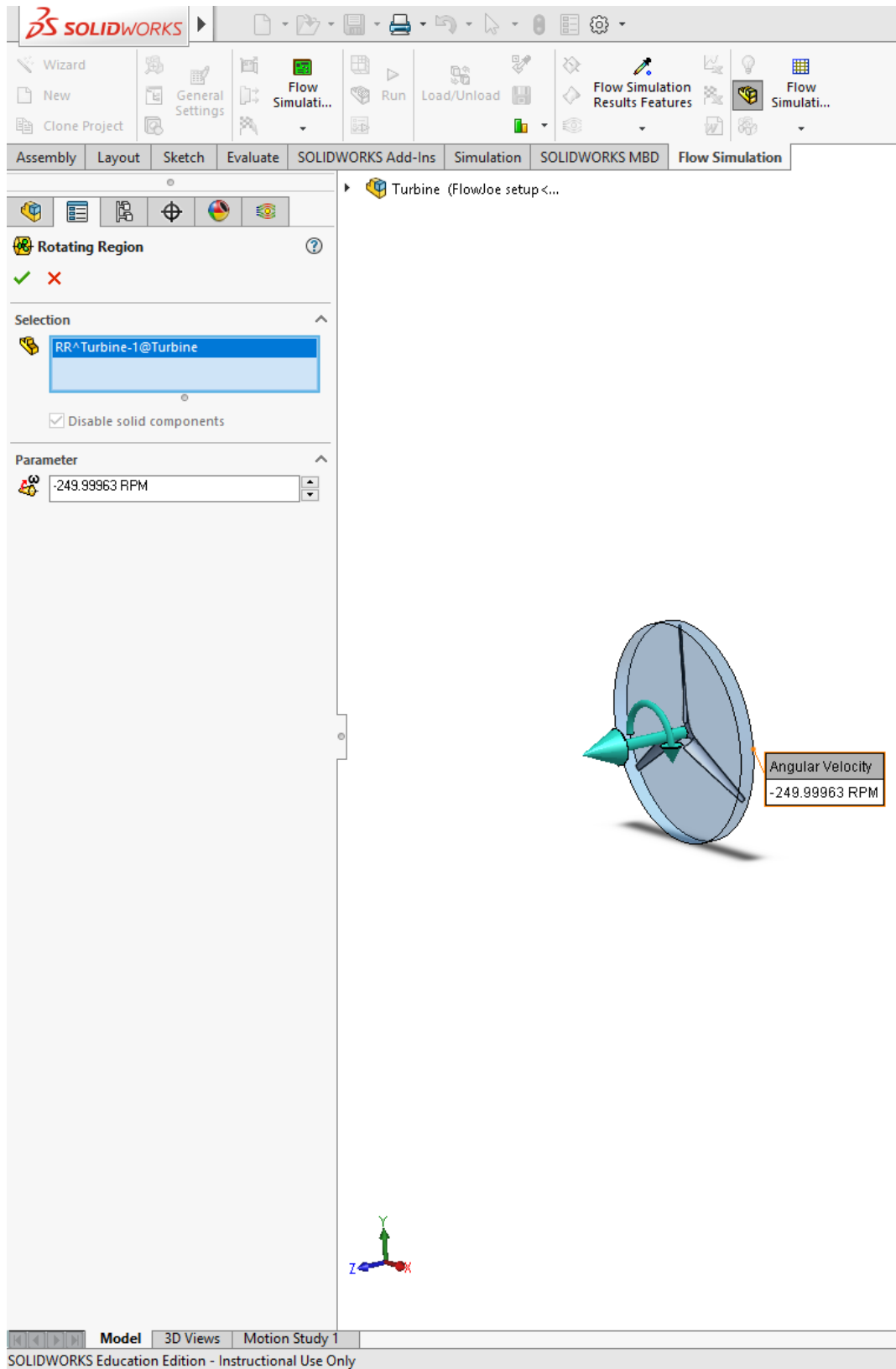The negative of the angular speed was inputted for each individual test. This is because the wind turbine test rig blades cannot be rotated in the simulation; therefore, it was necessary to rotate the air in the opposite direction [4].

We then set the three Boundary Conditions from the Insert Boundary Condition button, as seen in Figure 24 and Figure 26:
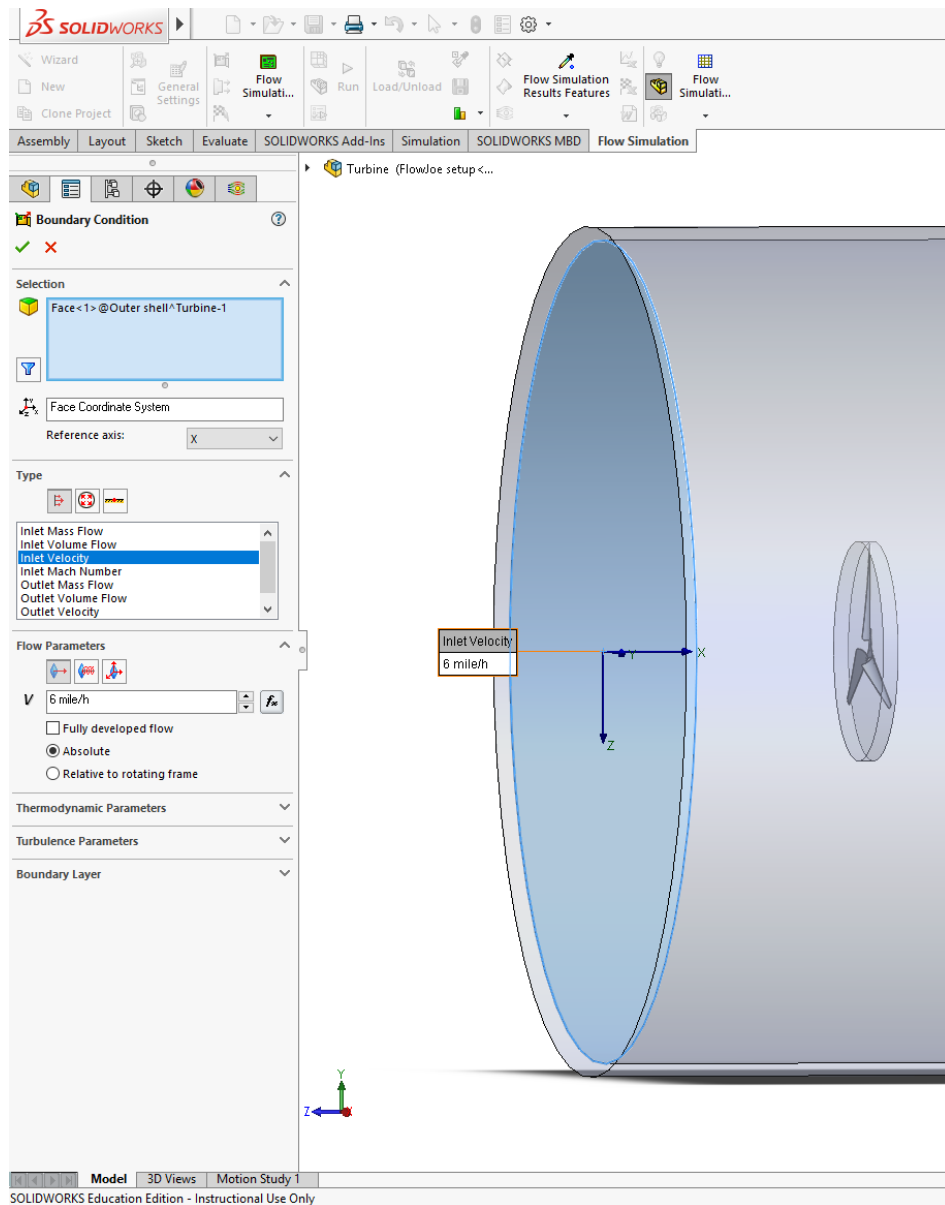
Figure 24 - Inlet Velocity Boundary Condition

The first type of boundary condition was identified as Inlet Velocity and Flow Parameters was set as normal to the face at the linear wind speed. The inside front face of the volume control (separated by the thin extrude) was selected because the fluid is flowing on the inside. In addition, an Environmental Pressure Boundary Condition was set for the back inside face of the volume control in order to allow the air in the simulation to flow out of the volume control (instead of recirculating), as seen in Figure 25:
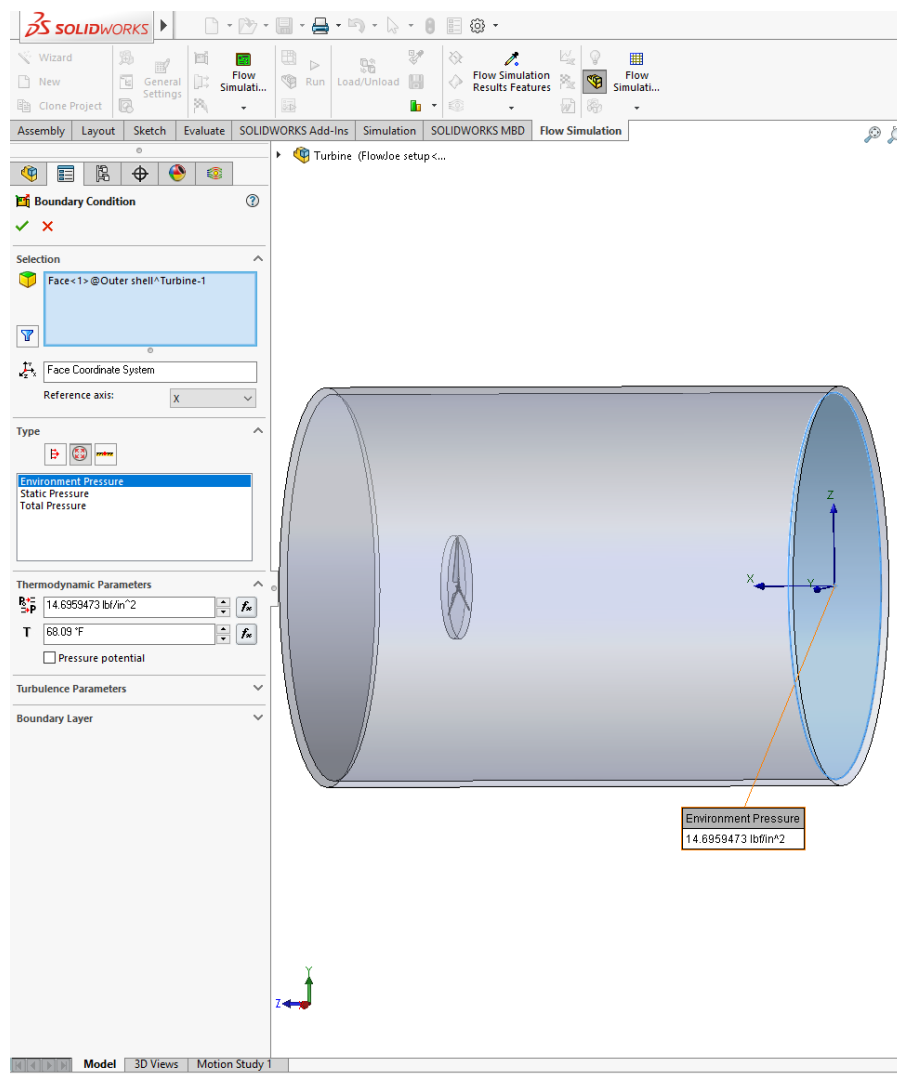
Figure 25 - Environment Pressure Boundary Condition

The second type of boundary condition was identified as Pressure Openings and Environment Pressure. Finally, an Ideal Wall Boundary Condition was set by selecting the entire inside lateral area, as seen in Figure 26:
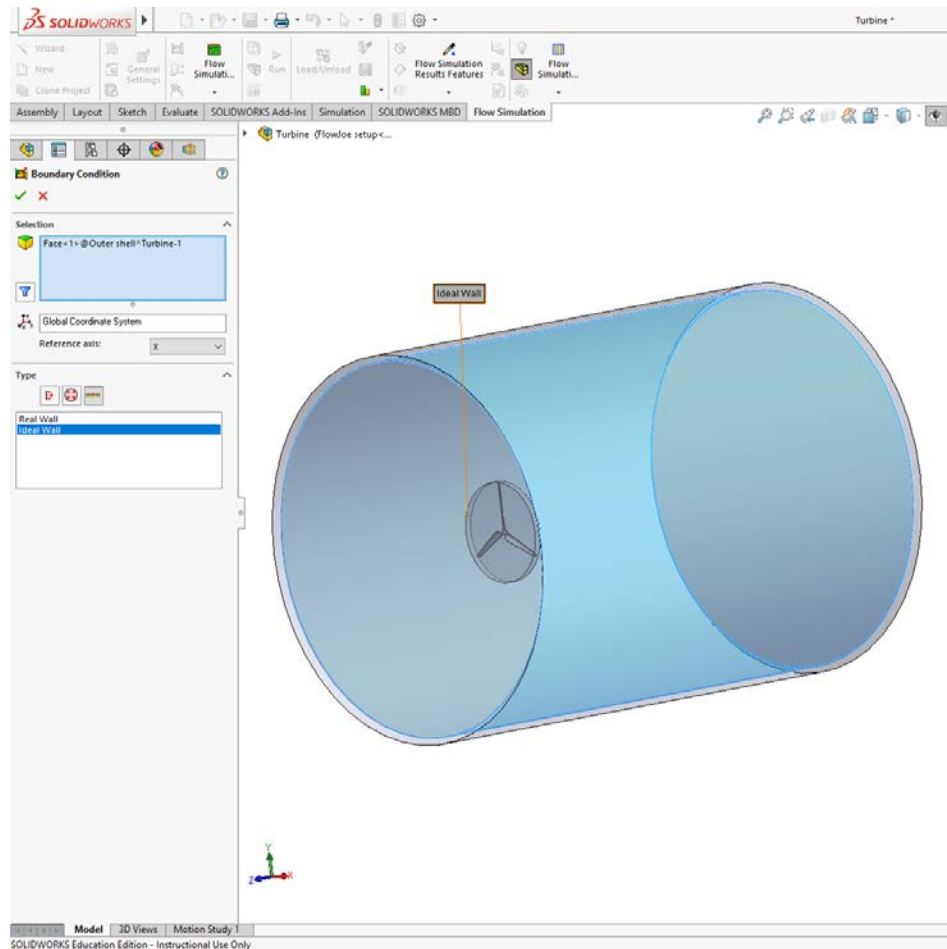
Figure 26 - Ideal Wall Boundary Condition

The third type of boundary condition was identified as Wall, specifically Ideal Wall. The Ideal Wall simulates outdoor conditions by making the conditions of the inner face of the volume control to be the same as the conditions of the outer face of the volume control (separated by the extrude) [4].

The next step is creating the mesh, which is important because it will help define how long it will take to run and the level of detail for each simulation. A mesh is like a window pane (a rectangle cut into four smaller rectangles), and refining cells by a level cuts each individual rectangle into four smaller rectangles. The first mesh that was established as a local mesh by right-clicking on mesh and selecting local mesh, as seen in Figure 27:
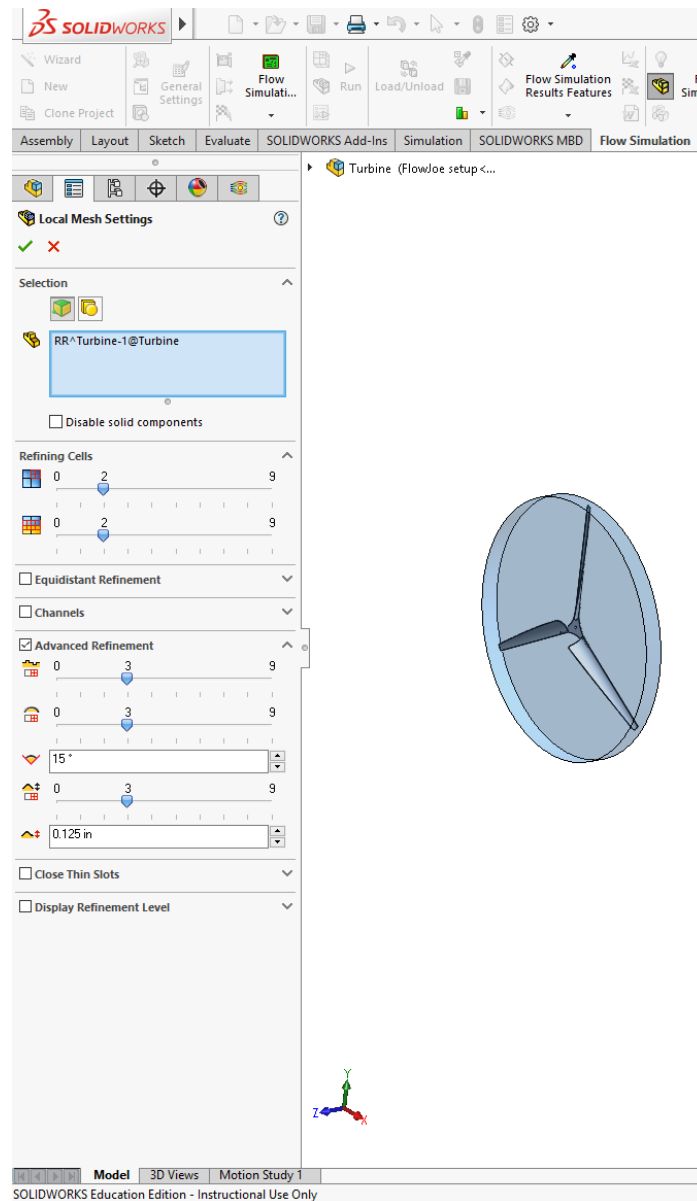
Figure 27 – Local Mesh 1

Under the selection title, the Reference button was selected so that the mesh could be established relative to the part of the CAD model. The part selected was the Rotating region. Refining Cells (both the Level of Refining Fluid Cells and the Level of Refining Cells at Fluid/Solid Boundary) were set to 2 because it used the smallest sized cells while allowing for an accurate mesh. Channels were unselected because they were not considered useful for our applications. Advanced Refinement allows for geometric features that further refine the mesh. For the first local mesh, the Small Solid Feature Refinement Level, the Curvature Level, and Tolerance Level were all set to 3. The Curvature Criterion was set to 15°. The Tolerance Criterion was set 0.125 inches because it was the thickness of the blades.

Local mesh 2 was designated as a region selection, which utilizes a shape to define the mesh, as seen in Figure 28:
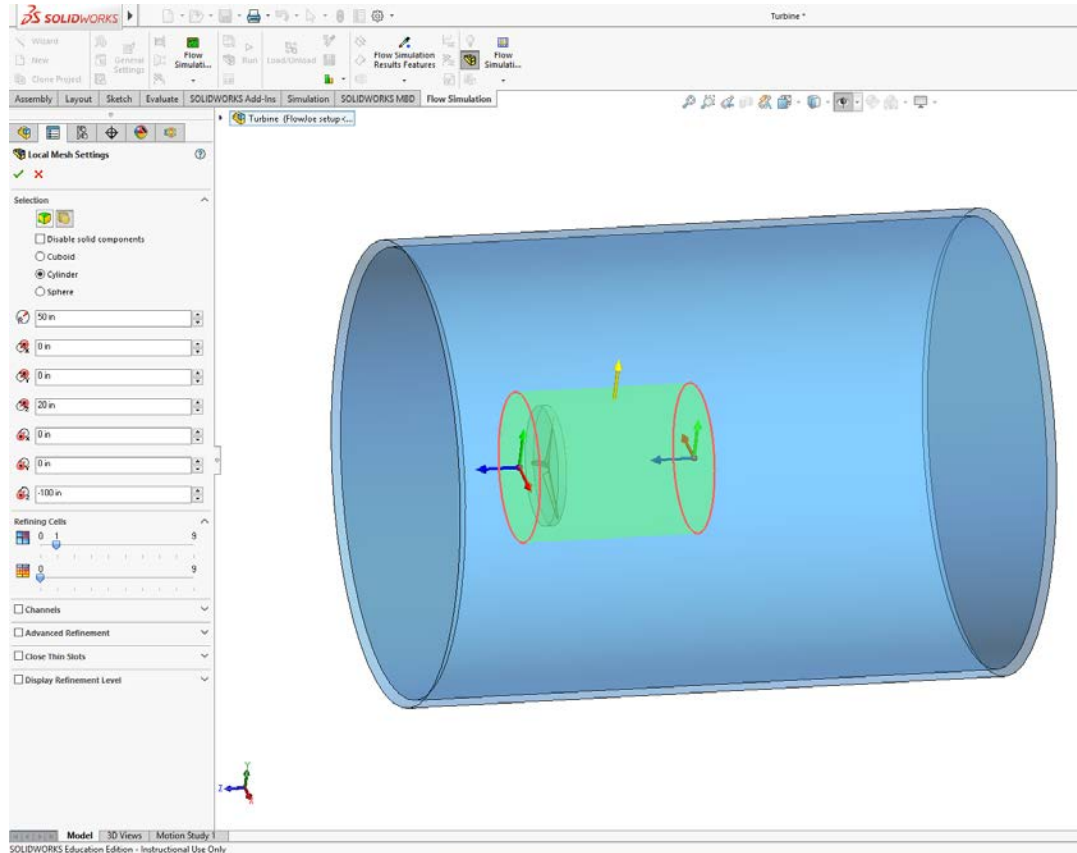
Figure 28 - Local Mesh 2

Under the selection title, the Region button was selected and identified as a cylinder, with a radius of 50 inches and a height of 120 inches. This local mesh is meant to take the global region and refine the mesh as it approaches the wind turbine test rig blades. Therefore, the Level of Refining Fluid Cells was set to 1 and the Level of Refining Cells at Fluid/Solid Boundary to 0. Channels and advanced refinement were not used for this local mesh.

Local mesh 3, seen in Figure 29, the local mesh associated with the wind turbine test rig blades, was a Reference selection, similar to local mesh 1.
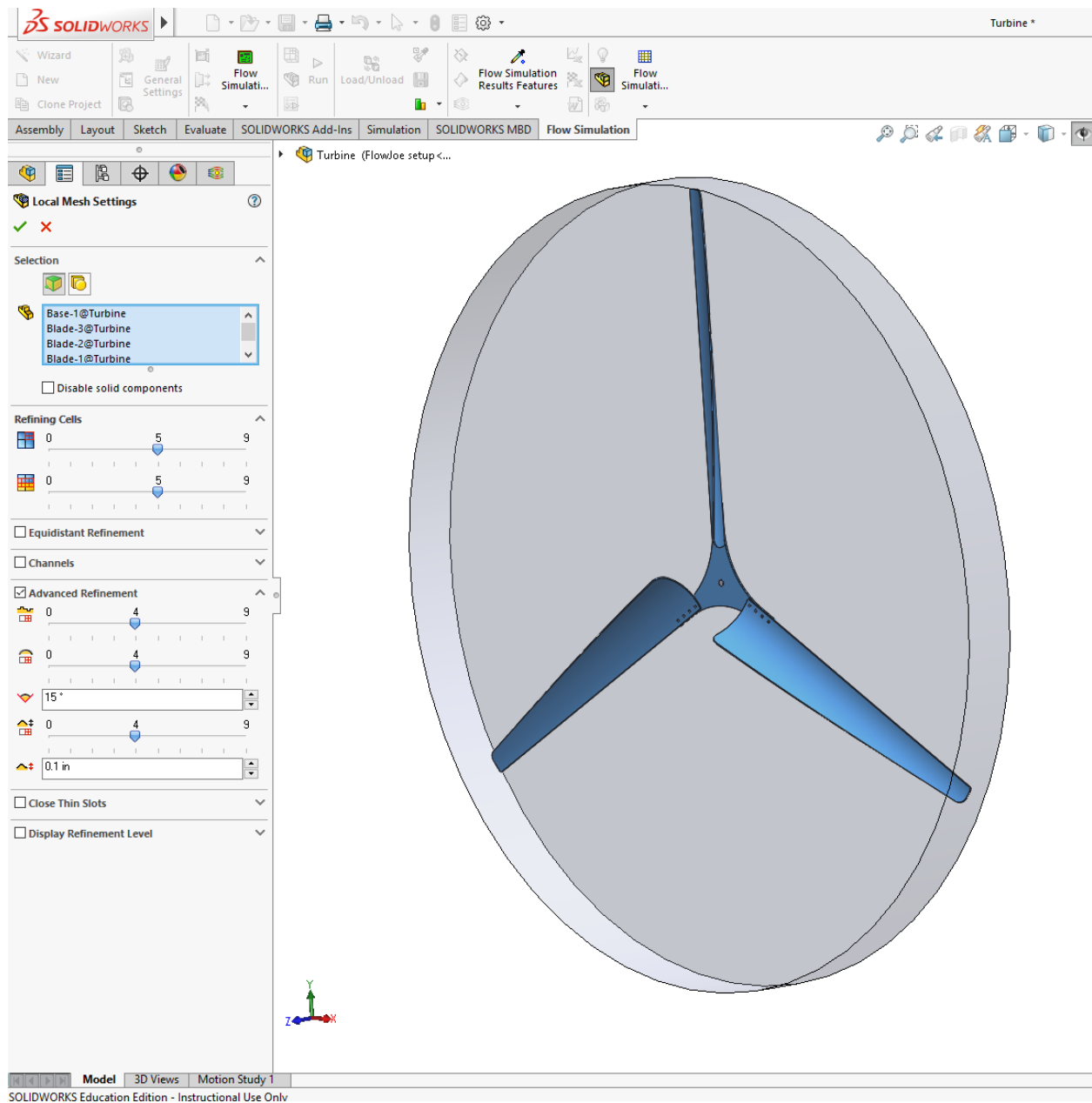
Figure 29 - Local Mesh 3

The parts selected were the wind turbine test rig blades and the base plate. The Level of Refining Fluid Cells and the Level of Refining Cells at Fluid/Solid Boundary were both set to 5.

For the Advanced Refinement, the Small Solid Feature Refinement Level, the Curvature Level, and Tolerance Level were all set to 4. The Curvature Criterion was set to 15°. The Tolerance Criterion was set 0.125 inches.

Local mesh 4 was also a Reference selection, selecting the faces and lateral area of the rotating region, as seen in Figure 30:

Figure 30 - Local Mesh 4

The purpose of local mesh 4 was to establish another boundary between local mesh 1 and the global mesh, which creates another layer of refinement. The Global mesh was set to the automatic type for ease of use and settings were set to the 7th level because it was the smallest cell size in the automatic type [4].

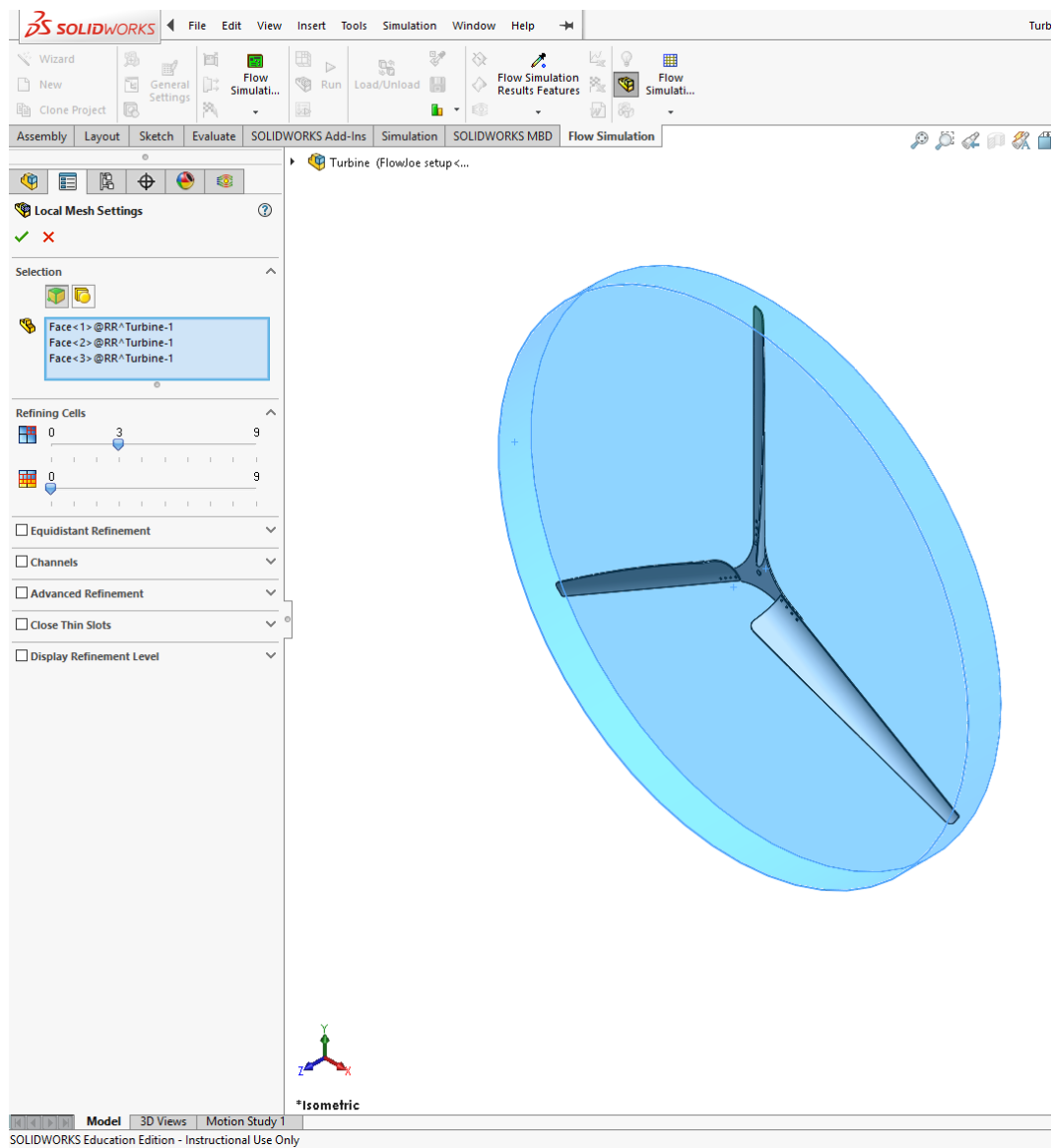After completing all the necessary meshes, goals were established for converging towards a solution and cutting down on computational time. The four-goal outputs of our wind turbine test rig were the torque value, the static pressure, the minimum wind velocity, and the fan volumetric flow rate. The torque value, the main objective of the flow simulation, was set as a surface goal, as we were attempting to ascertain the amount of torque applied to the surface of our blades. In order to properly simulate a free-flowing wind turbine test rig, for a given wind speed we hoped that our estimate of the RPM would result in a torque value of 0. If this did not happen, we would go back and input a different RPM estimate until we achieved our objective. The static pressure was set as a global goal to find the average static pressure. This value was simply found for convergence and was not critical. The minimum wind velocity was set as a global goal. The minimum was found because all inputted wind velocities were negative due to the orientation of the wind turbine test rig blades (and so finding the minimum was essentially finding the absolute maximum). The purpose of this goal was simply to have a way to gauge the accuracy of results. Finally, the Fan Volumetric Flow Rate was established at the request of Joe Galliera was not critical for our experiment [4].

In order to proceed with the flow simulation, we set up a "What If" analysis parametric study (not goal optimization). We chose a parametric study instead of a regular run (the other option) because the regular run was giving us inconsistent results due to a bad mesh.

Furthermore, a parametric study is easier to set up and run [6]. A "What If" analysis shows what would happen given that we change a certain variable as seen in Figure 31:
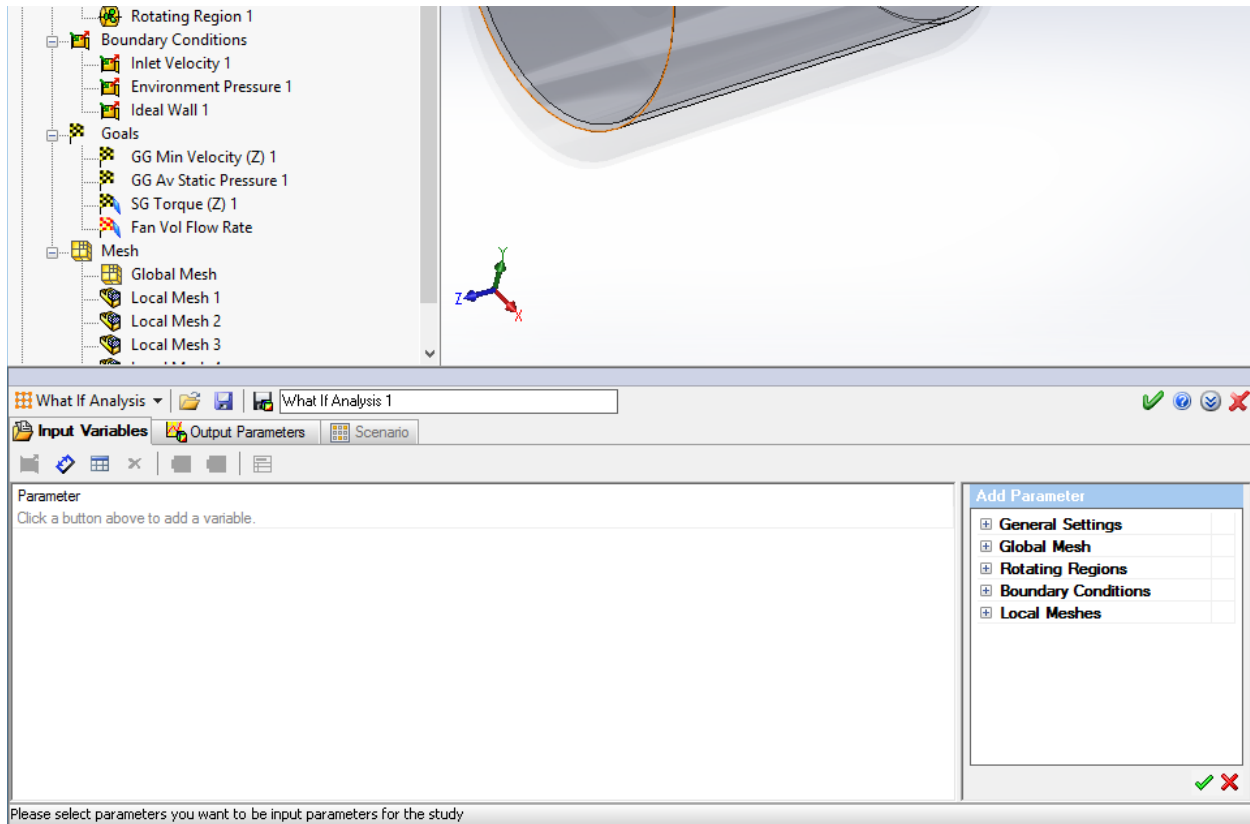
For the purposes of our wind turbine test rig, we chose to change the angular velocity (RPM) to see what would happen with the torque on the wind turbine test rig blades. To begin, initial conditions of velocity in the Z direction were established due to the orientation of the CAD model by going to General settings and clicking on Initial conditions. Then, by going to the Rotating region section, the angular velocity was selected. To establish Boundary conditions for

the parametric study, the environment pressure was set and the inlet velocity was made to be

normal to the face. These setting can be seen in Figure 32:

Figure 32 - Input Variables for "What If" Analysis

The Level of Refining Fluid Cells and the Level of Refining Cells at Fluid/Solid

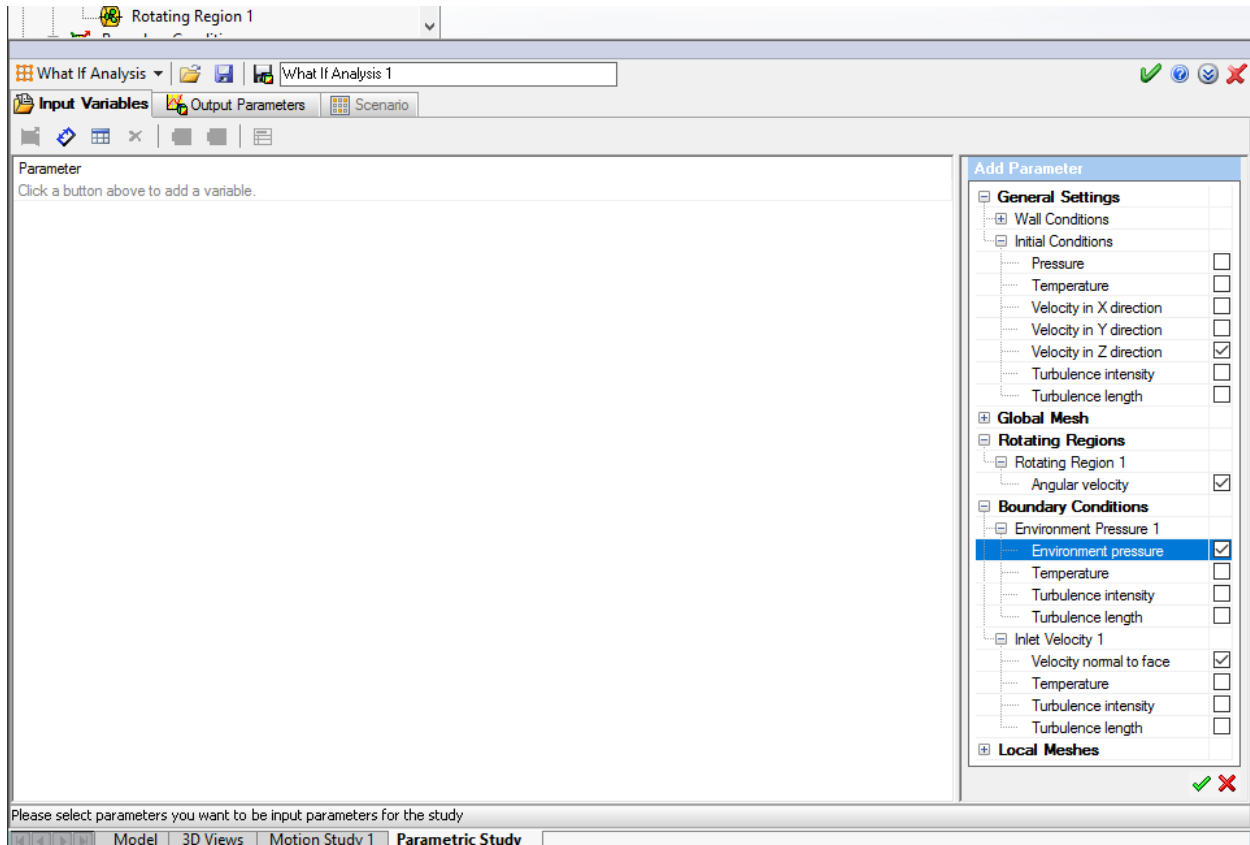Boundary of Local Mesh 1-4 were considered for the parametric study as seen in Figure 33:
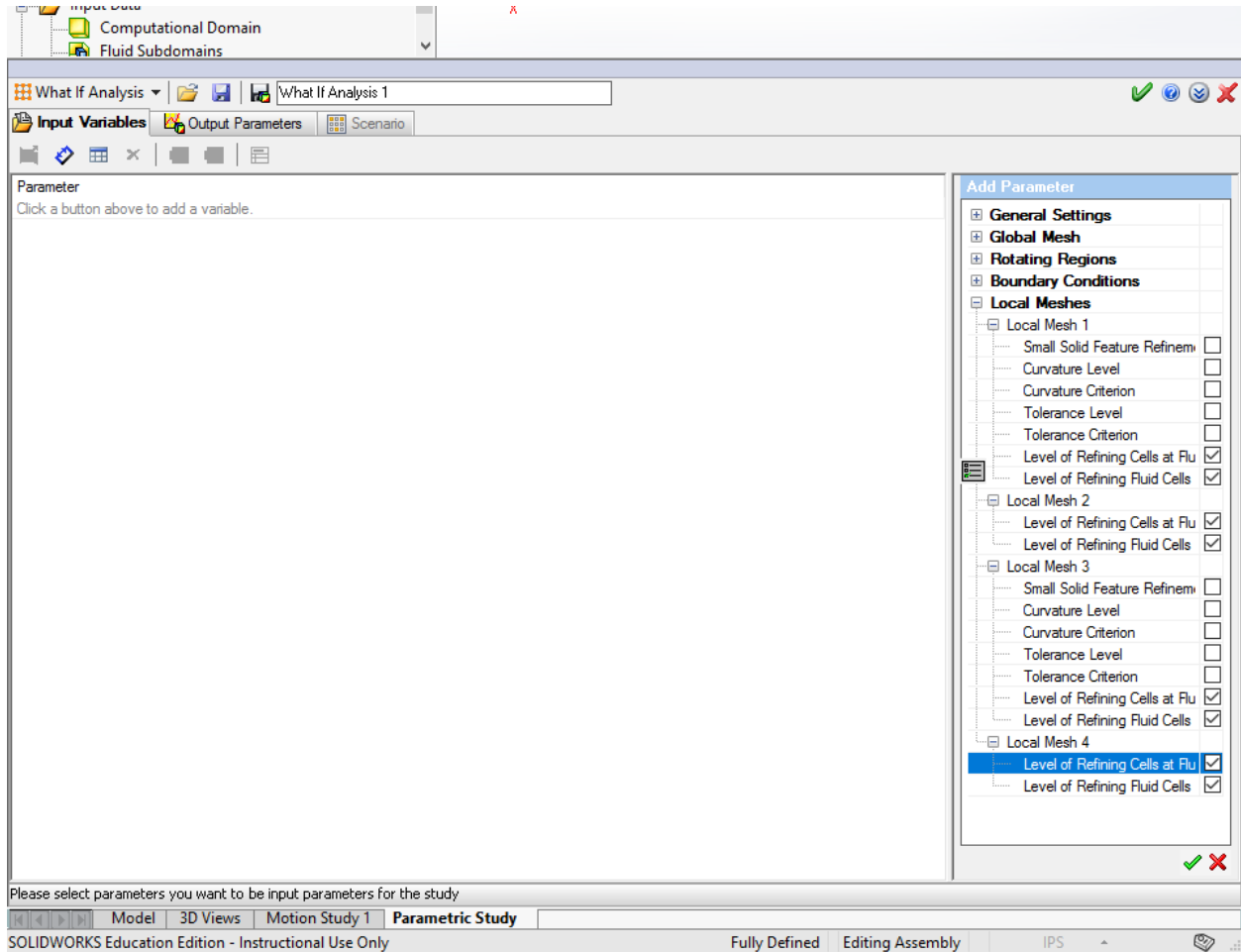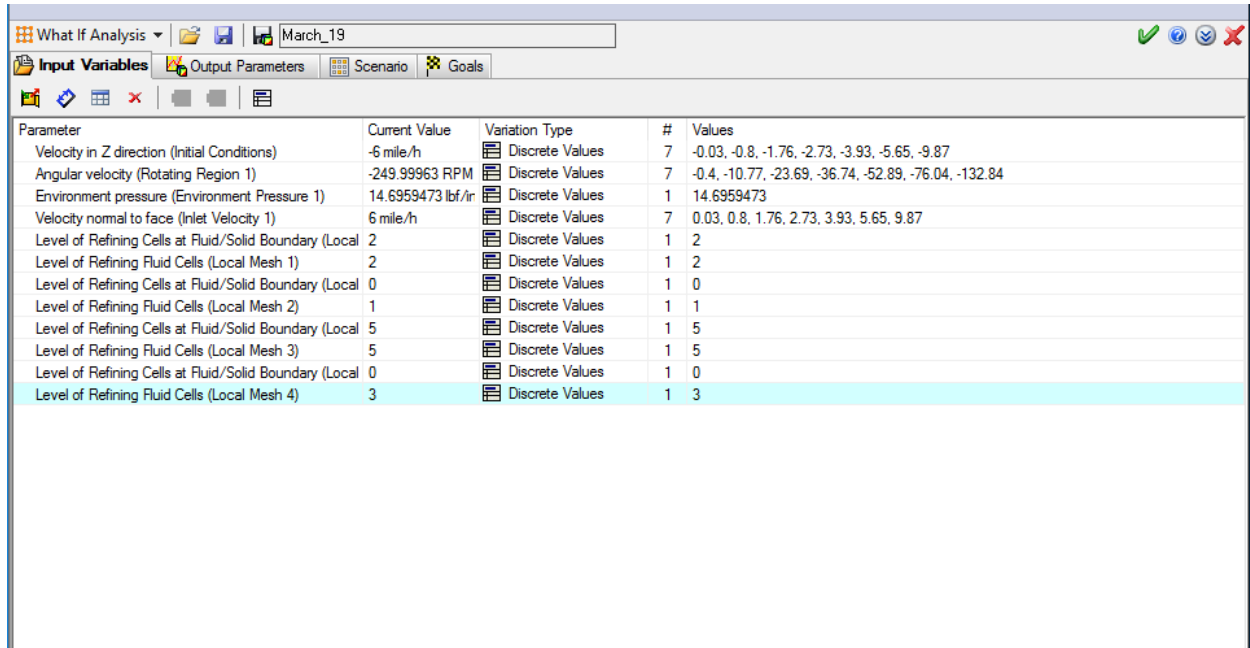
Figure 33 - Local Meshes for "What If" Analysis

Multiple values were entered into the initial conditions, rotating region and inlet velocity

as seen Figure 34:

Figure 34 - Parameter Values Entered

Initial Condition velocity in Z-direction should be the negative value of the Inlet

Velocity due to the orientation of the model. Output variables were designated as the minimum

wind velocity, torque volume, and the volumetric flow rate goals as seen in Figure 35:
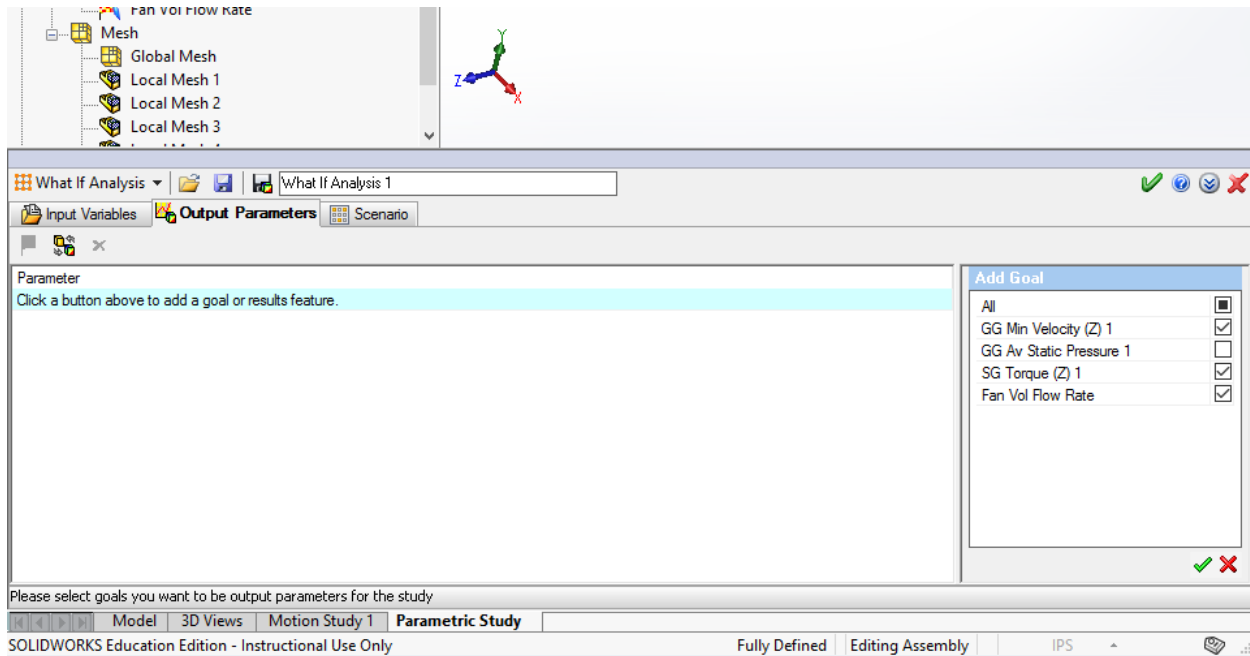
Figure 35 - Output Parameters for "What If" Analysis

The scenario section comes up with all possible combinations of the variables. This

functionality allowed us to sort through the combinations and select the ones that pertained to

our objectives [4].

4.2 Flow Simulation Final Results

From the SolidWorks Flow Simulation, we inputted data about our wind turbine test rig blades to calculate power output if we harnessed its power. Table 1 shows the torque values at different RPMs and wind speeds in inch-pounds:

Table 1 - Raw Data Output From Flow Simulation

		Wind Speed			
RPM	**0**	**6**	**9**	**11**	**MPH**
10	0	-6	-13	-19	
50	0	-8	-13	-19	
75	0	-6	-17	-23	
100	0	-3	-16	-26	Units:
125	0	2	-12	-24	in*lb
150	0	8	-7	-19	
250	0	42	29	16	
1000	0	828	818	810	

(Rotation speed label spans rows)

Positive values of torque mean that the wind turbine is a fan and negative values of torque mean that the wind turbine is a generator. As such, positive values of torque will become 0 because the wind turbine could be built such that it shuts off when it starts consuming power. Table 2 shows the true torque values:

Table 2 - True Torque Values of Flow Simulation

		Wind Speed			
RPM	**0**	**6**	**9**	**11**	**MPH**
10	0	-6	-13	-19	
50	0	-8	-13	-19	
75	0	-6	-17	-23	
100	0	-3	-16	-26	Units:
125	0	0	-12	-24	in*lb
150	0	0	-7	-19	
250	0	0	0	0	
1000	0	0	0	0	

(Rotation speed label spans rows)

As previously stated, power in a rotational setting is the product of torque and angular velocity and a conversion factor to obtain the units of Watts. Table 3 converts the torque values at their given RPMs to the corresponding power outputs in Watts:

Table 3 - Power Output of Flow Simulation

		Wind Speed (MPH)			
		0	6	9	11
	10	0	-1	-2	-2
	50	0	-5	-8	-11
	75	0	-6	-15	-21
Rotation	100	0	-3	-19	-30
Speed (RPM)	125	0	0	-18	-35
	150	0	0	-12	-34
	250	0	0	0	0
	1000	0	0	0	0
Max Power		0.0	5.7	19.2	35.0

Output Units: Watts

At the bottom of Table 3, there is the predicted maximum power. This maximum power was calculated through the power in the wind equation while incorporating the Betz limit and some efficiency.

4.3 Flow Simulation Free-Spinning Analysis

Previously we have completed data for wind speeds at 6 MPH, 9 MPH, and 11 MPH. We only have completed data at these wind speeds because greater wind speeds have such low probabilities. Then, we graphed RPM versus Torque at given wind speeds and we found that the graphs produce quadratic trends. For our eight data points, at each wind speed, we obtained R^2 values of 0.9976, 0.9932, and 0.9745 respectively. Figure 36, Figure 37, and Figure 38 show the graphs at each wind speed:
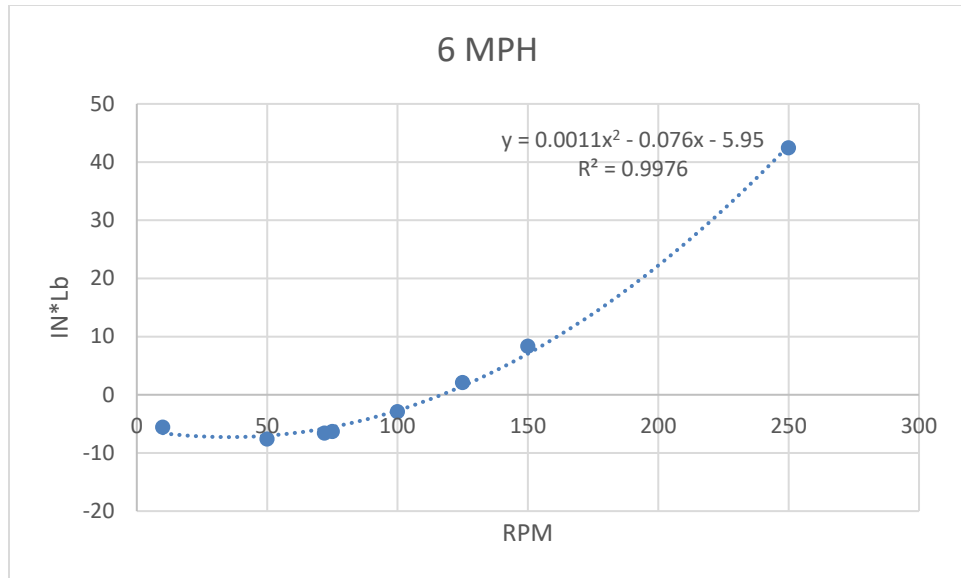
Figure 36 - 6 MPH Graph

Figure 37 - 9 MPH Graph

11 MPH

$y = 0.0014x^2 - 0.2378x - 14.41$
$R^2 = 0.9745$
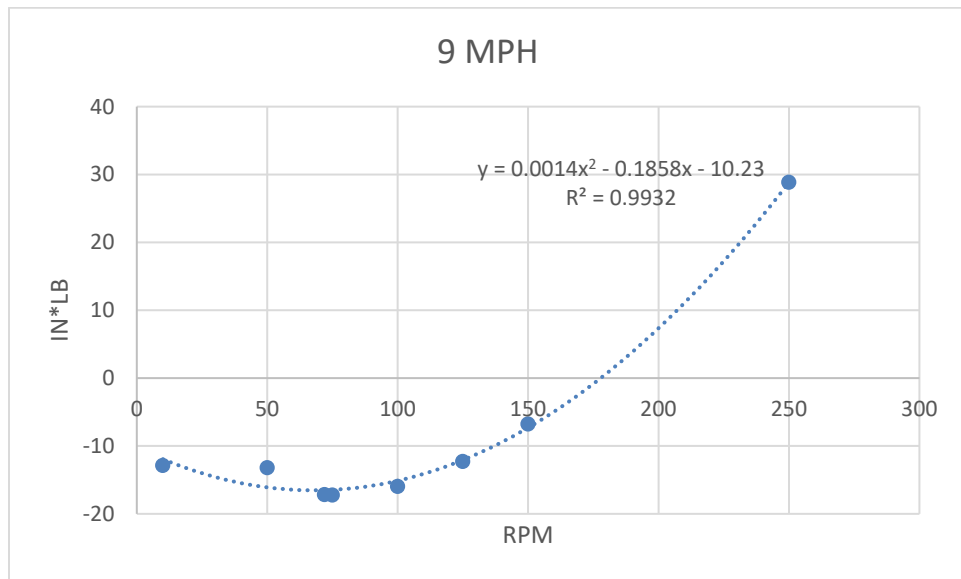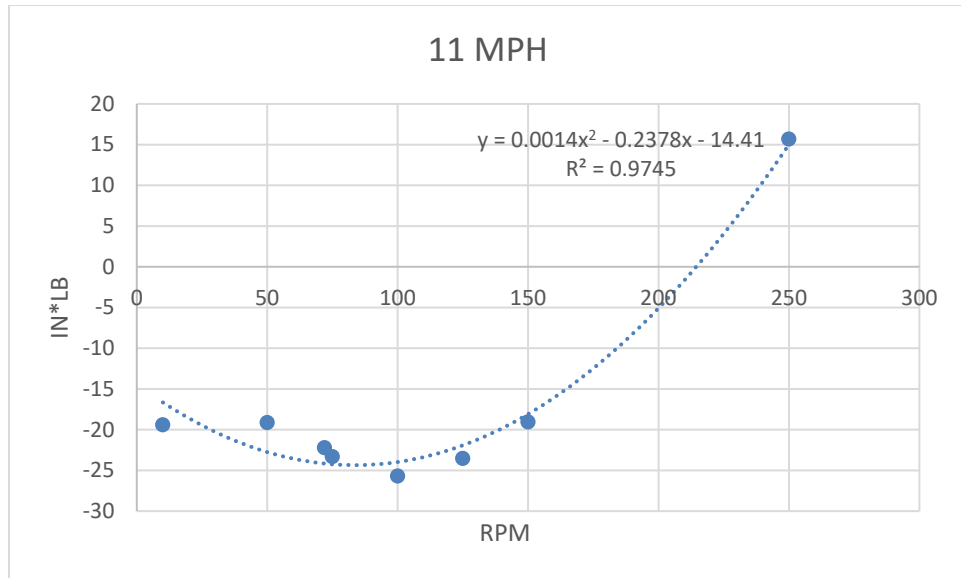
Figure 38 - 11 MPH Graph

Solving for the positive, real roots of the three quadratic equations, we found the estimated RPM for a free spinning turbine to be 116, 175, and 212 RPM for 6, 9, and 11 MPH respectively. We then used these RPMs and wind speeds in SolidWorks Flow Simulation. The torque outputs were approximately 0.06, 0.37, and -0.30 inch-pounds respectively. 9 MPH and 175 RPM had the torque of the highest magnitude. From 175 RPM we added and subtracted 3 RPM at 9 MPH to see if we could achieve a torque of smaller magnitude. We obtained 1.1 inch-pounds at 178 RPM and -0.53 inch-pounds for 172 RPM. Both of these yielded larger magnitudes of torque, so our original estimation was the best. With the original torque output simulations, we created Figure 39, the graph comparing RPM vs wind speed in a free spinning state:

56
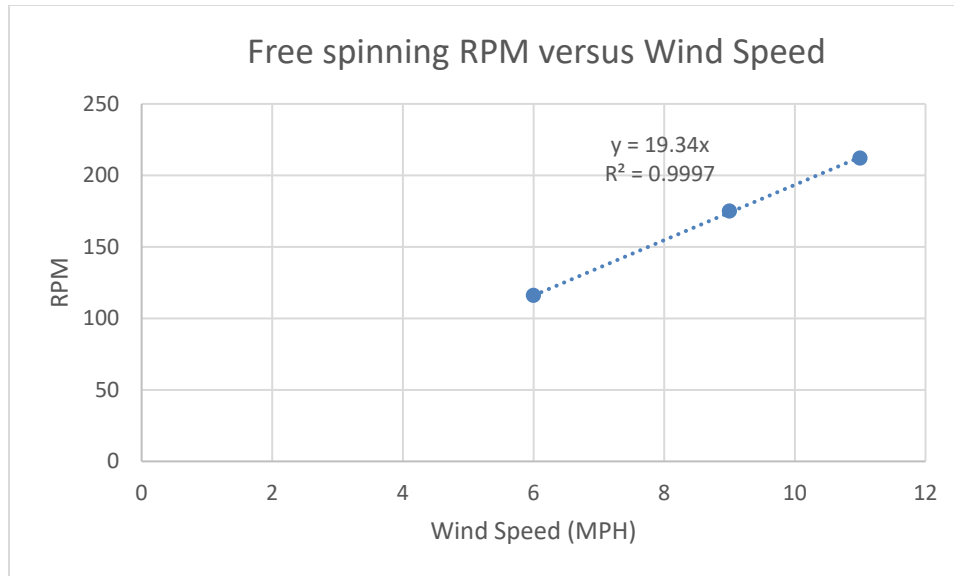
Figure 39 - Free Spinning RPM versus Wind Speed

For the trend line, we fixed the intercept at (0,0) because at 0 MPH wind speed, there is 0 rotation. In this case, the trend was clearly linear and produced a relationship of 19.3 RPM for each increase in 1 MPH. We will be using this trend line to predict what the RPM of the wind turbine test rig will be at each wind speed.

From adjusting the RPM at 9 MPH as mentioned above, when we reduced it by 3 RPM the torque dropped by 0.9 inch-pounds. When we increased the RPM by 3 the torque increased by 0.75 inch-pounds. In the reverse situation when we increase wind by 2 MPH but keep RPM constant the torque increases by roughly 5 to 15 inch-pounds. Due to these wind turbine blades, there will be a fair bit of inertia. A sudden change in wind speed will not cause a drastic change in RPM because of the inertia. Therefore, we have to care about the change in wind speed producing torque rather than a changing RPM to analyze our 0-torque range for free spinning. Given that our furthest data point from 0 is 0.37 inch-pounds, the above data, and adjusting the

RPM at 9 MPH, we believe that this point near perfectly depicts the free-spinning state of a wind turbine.

4.4 Flow Simulation Maximum Power Analysis

In addition to the free-spinning state, we also found that it would be beneficial to determine a trend line of wind speed vs RPM for the maximum power point of the wind turbine test rig. We started using the data from Section 4.2. In particular, Table 3 shows the maximum power at given RPM and wind speeds. To begin, we produced the graphs of 6, 9, and 11 MPH of RPM vs Power to determine their local minimums (which would be the maximum powers and respective RPMs for each wind speed). These graphs can be seen in Figure 40, Figure 41, and Figure 42:

The graph, titled "6 MPH", plots Power (Watts) on the y-axis (ranging from -10 to 20) versus RPM on the x-axis (ranging from 0 to 160). The fitted trend line equation is $y = 2\text{E-}05x^3 - 0.0011x^2 - 0.0764x$ with $R^2 = 0.9995$.
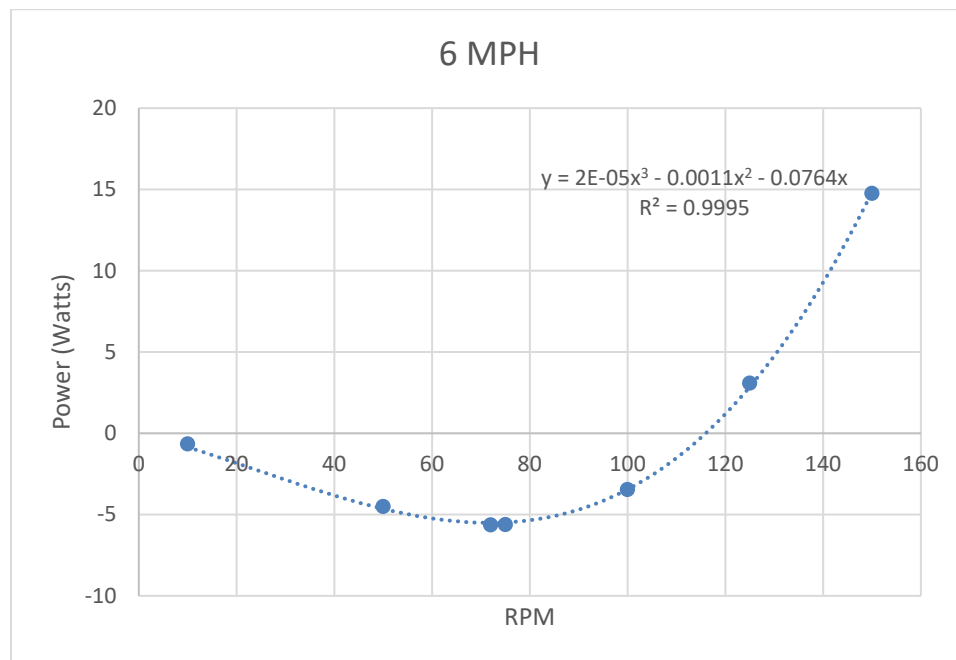
Figure 40 - 6 MPH Graph, RPM vs Power
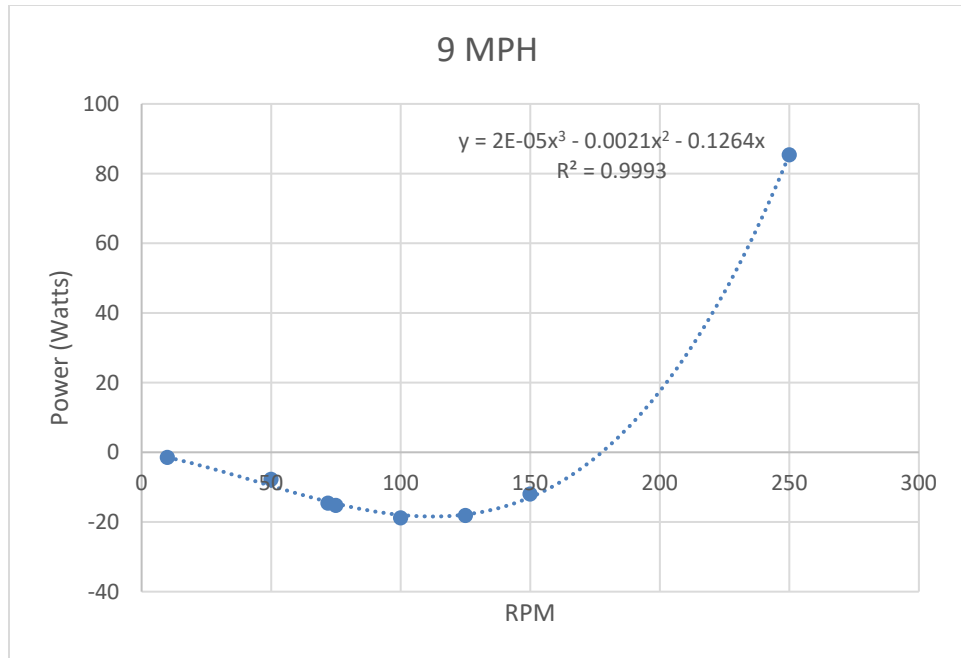
Figure 41 - 9 MPH Graph, RPM vs Power
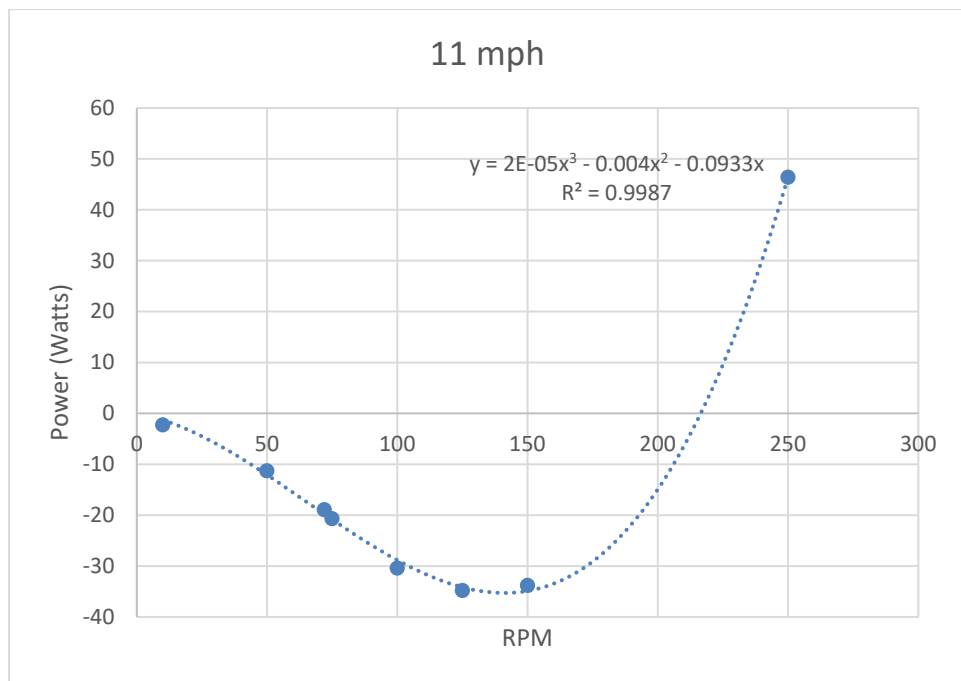
Figure 42 - 11 MPH Graph, RPM vs Power

The three graphs gave us three data points to plot for the maximum power trend line.

Unfortunately, unlike the free-spinning state, these three points were not enough to make the

trend line. Because of this, we decided to retrieve more data. We used 3 MPH and 13 MPH and produced their perspective graphs, as seen below in Figure 43 and Figure 44:
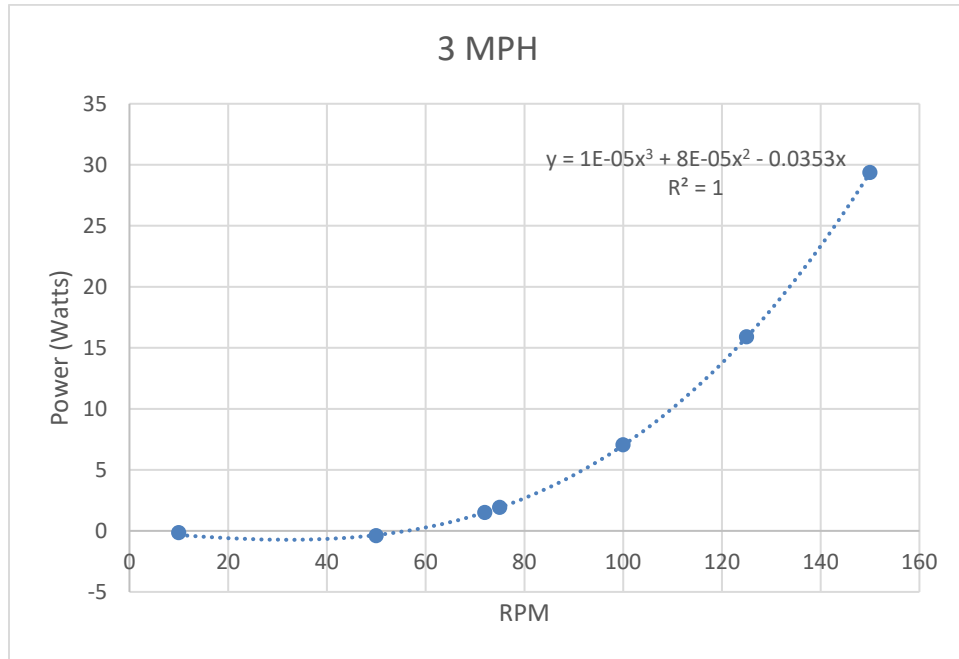
Figure 43 - 3 MPH Graph, RPM vs Power
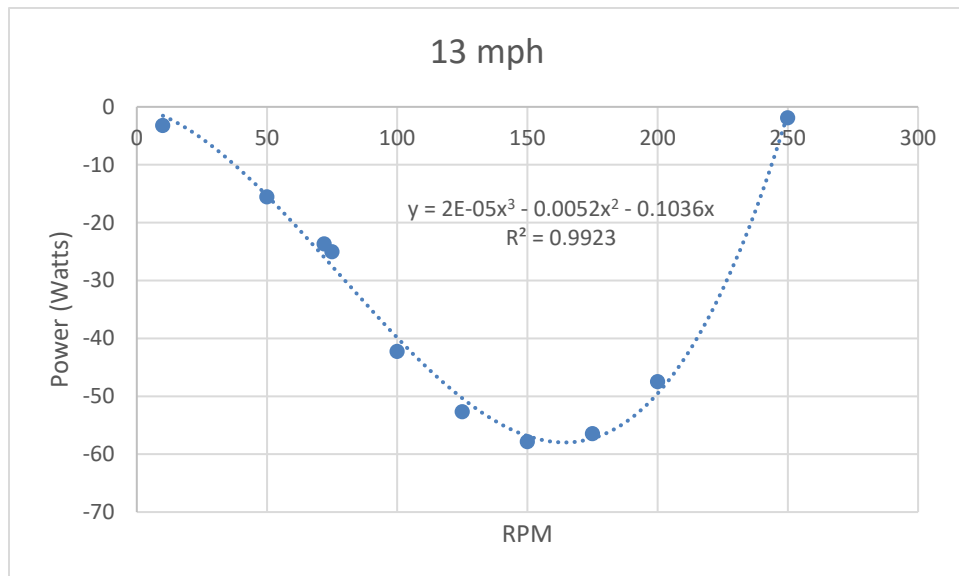
Figure 44 - 13 MPH Graph, RPM vs Power

With these two additional graphs, we were able to produce two more data points for the trend line. Together, the five points were able to make a clear trend line, as seen in Figure 45:
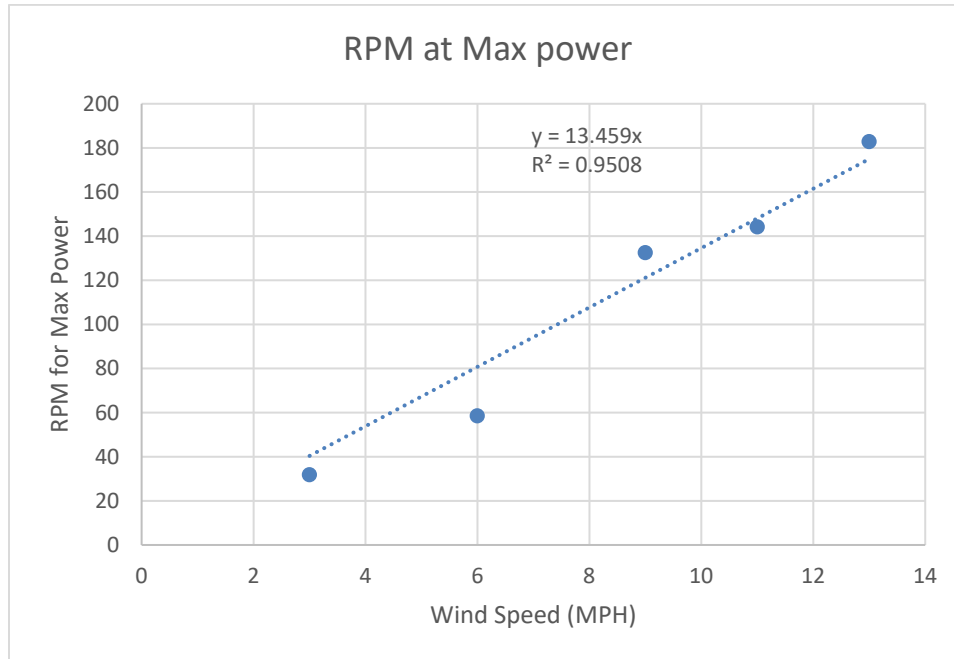
Figure 45 - Maximum Power Graph

Once again, for the trend line we fixed the intercept at (0,0) because at 0 MPH wind speed, there is 0 rotation. In this case, the trend was clearly linear and produced a relationship of 13.459 RPM for each increase in 1 MPH. We will be using this trend line to predict what potential power the wind turbine test rig could produce at all wind speeds.

4.5 Flow Simulation Conclusion

From the analysis of our SolidWorks Flow Simulation data, we were able to obtain wind speed versus RPM trend lines for max power and free-spinning states of a wind turbine. This can be seen in Figure 46 in a single graph:
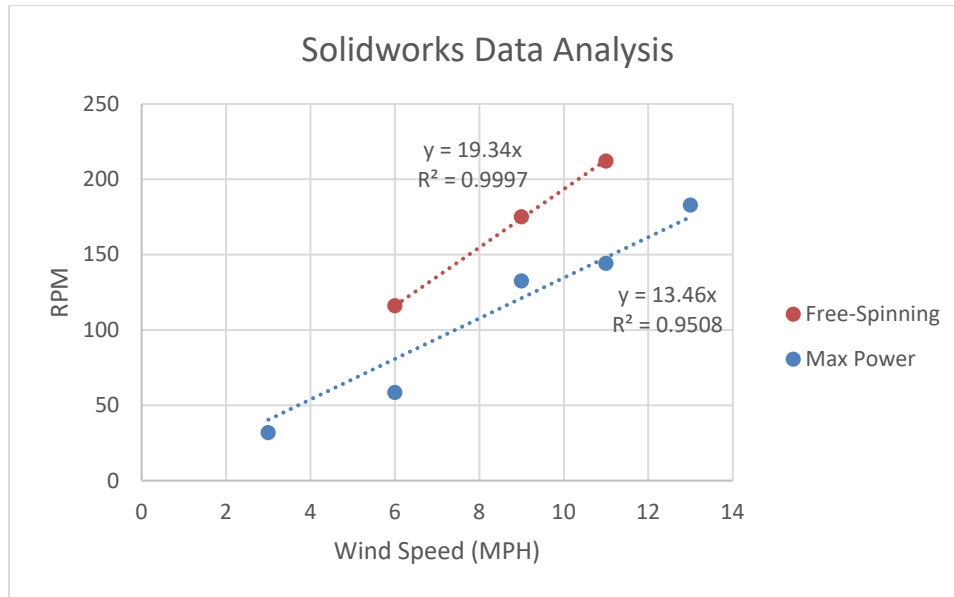
Figure 46 - SolidWorks Data Analysis Trendlines

By dividing the slope of the max power trendline by the slope of the free-spinning trend line, a value of approximately 0.6996 is obtained. Cubing this number and then taking the square root of it would yield a value of 0.58, which is very close to the Betz limit. Given that the power in the wind is proportional to the cube of the wind speed and rotational kinetic energy is proportional to the square of angular velocity, we do not believe that this is a coincidence. If this is true for three bladed systems, it would eliminate the need for CFD or rigorous field testing data to determine the max power. By testing a wind turbine in free spinning state and multiplying its trendline by 0.6996, one could potentially obtain the max power trendline. This would save a lot of time and effort. Another MQP could do more testing with different blade geometry to see if our hypothesis is true or not.

5.0 Wind Turbine Test Rig

After completing the flow simulations, it became possible to analyze the results and compare it to the data that we obtained from the wind turbine test rig. We also wished to determine the minimum amount of time required to have a sample size that would be deemed large enough to obtain an accurate average wind speed.

5.1 Wind Probability

As previously mentioned, power produced from wind is proportional to the cube of the wind speed. As such, ascertaining actual power output of the wind turbine test rig requires extensive wind data collection. We are collecting wind data to compare it to RPM of the wind turbine test rig and to figure out how long it would be necessary to obtain an accurate sample size.

A wind speed sensor (also known as an anemometer) was purchased for these reasons. Initially, we narrowed down our options to the Inspeed Vortex Wind Speed Sensor and the Ambient Weather WS-0900-IP Wireless Internet Remote Monitoring Weather Station. We chose the Inspeed Vortex Wind Speed Sensor because it outputs a pulse for every revolution (a linear relationship of 1 pulse/second to 2.5 MPH) at small enough intervals [7]. The Ambient Weather WS-0900-IP Wireless Internet Remote Monitoring Weather Station only produces a graph of its collected data and does not show data points that we need. It also only has intervals from day to day, which are too long for our purposes [8].

In addition, to make use of the Inspeed Vortex Wind Speed Sensor, an ESP8266 was programmed to receive wind data from the anemometer. The ESP8266 connects to Wi-Fi and logs data at 10-second intervals to a server in Northern Virginia. The ESP8266 counts the

number of times the anemometer makes a full rotation in a 10-second interval and then divides

that number by 10 to obtain the average number of rotations per second. Since 1 rotation/second

(Hz) is equivalent to 2.5 MPH, the average number of rotation can be converted into MPH by

multiplying it by 2.5. We have a website that can access the server, giving us live, up to date

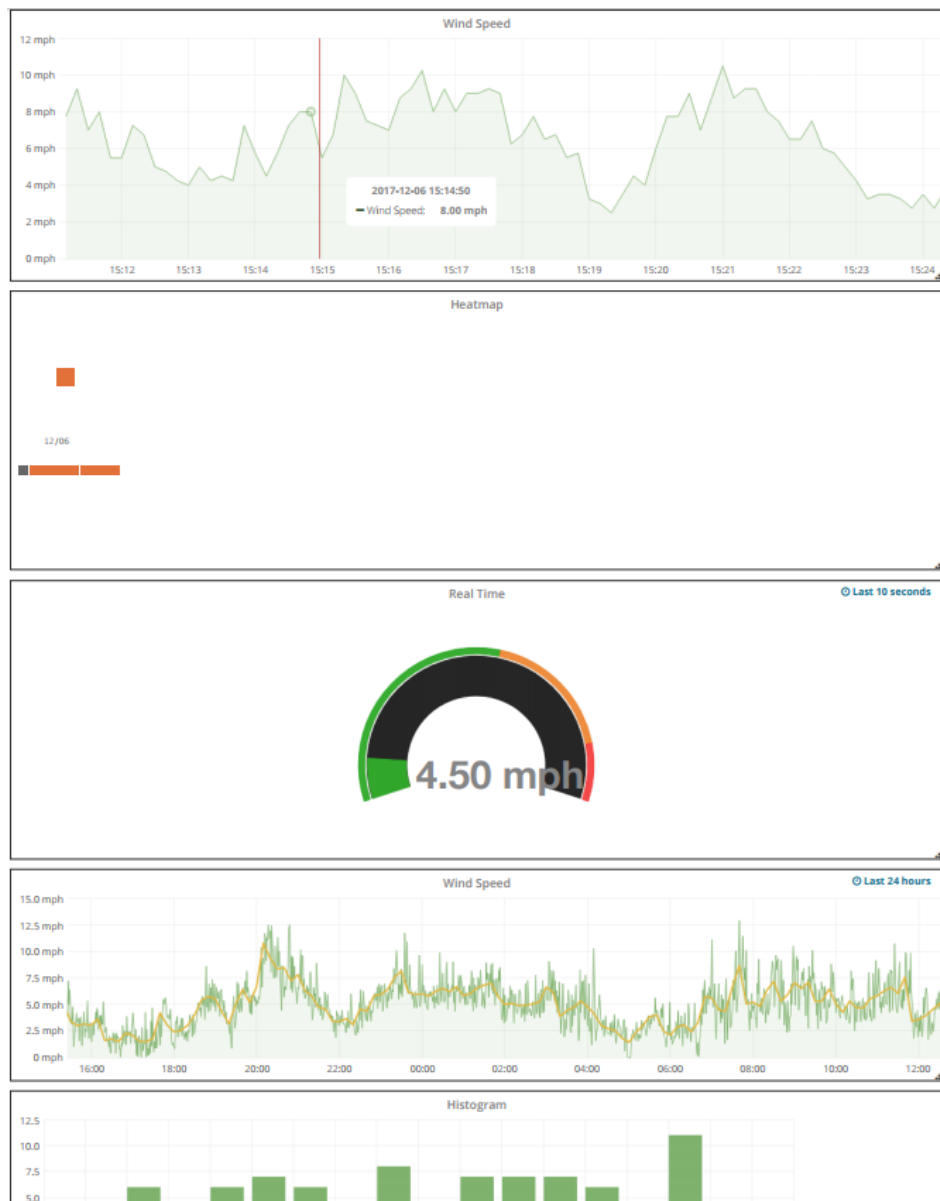information on the wind speed, as shown in Figure 47:

Figure 47 - Wind Speed Data Collection

We also had another ESP8266 on the wind turbine test rig that collected data through a Hall Effect sensor. Like the anemometer ESP8266, it sends data every 10 seconds. Each produced its own set of data. Because of this, it was necessary to match up the data sets by timestamp.

5.2 Wind Data Collection

We have collected 1,286,021 wind speed data points since September! For the SolidWorks analysis, we created 10 different equally-sized divisions. Table 4 shows maximums, minimums, average wind speed of the division, and estimated RPMs using the equation from Figure 46:

Table 4 - 10 Divisions Table (Please note: anemometer's smallest interval is 0.25 MPH)

Section	1	2	3	4	5	6	7	8	9	10	
Low speed of section	0	0	0	0	0.25	1.25	2.25	3.25	4.75	6.75	
High speed of section	0	0	0	0.25	1.25	2.25	3.25	4.75	6.75	36.75	Units: MPH
Average (mean) input	0	0	0	0.0	0.8	1.8	2.7	3.9	5.7	9.9	
estimate input RPM	0	0	0	0.6	15.4	33.9	52.5	75.6	108.7	189.9	Units: RPM

We can see here that roughly 1/3 of the time there is no wind. From a power output standpoint, which is proportional to the cube of the wind speed, as long as there are high wind speeds for a proportion of the time, there will be sufficient output. Figure 48 shows the wind speed versus percentage of total:
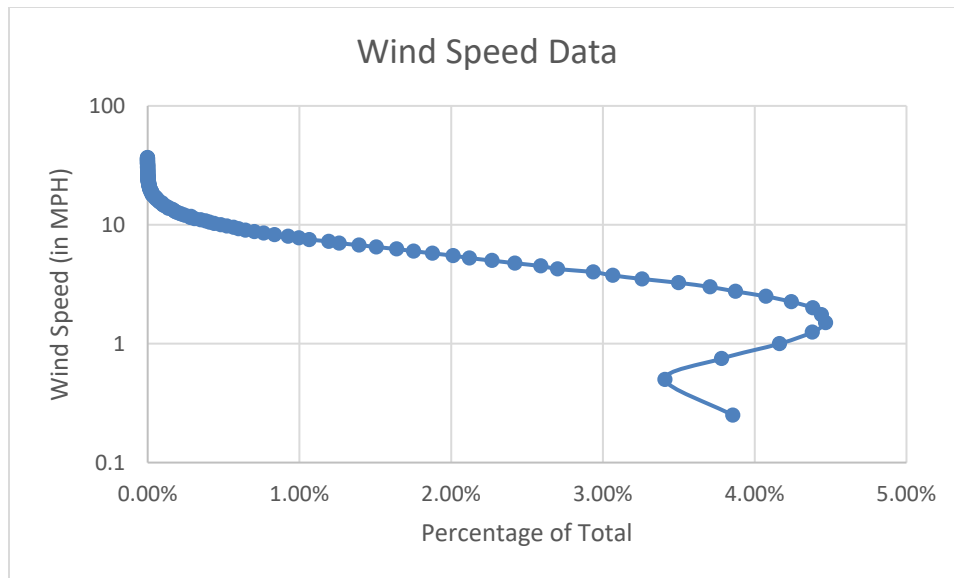
Figure 48 - Wind Speed Vs Number of Percentage of Total

5.3 Wind Data Sample Size

One of our objectives was to determine a minimum amount of time for wind data collection. Figure 49 shows a graph with a horizontal line that represents the total average of the data collection and a curve which represents the running average trend:
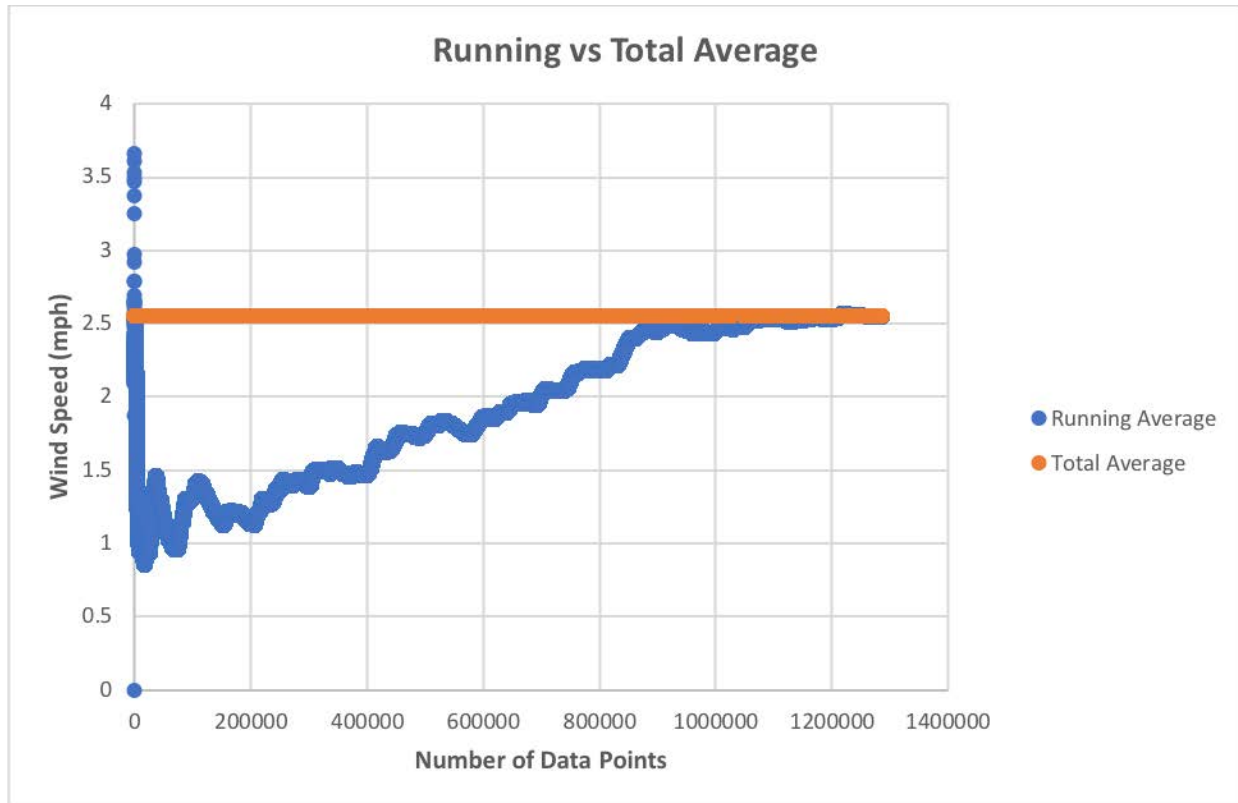
Figure 49 - Running Average vs Total Average

The running average trend approaches the total average and where the two meet is the necessary minimum sample size. It can be seen that this occurs at approximately the 825,000[th] increment. This would correspond to 3.2 months given that each data point occurs roughly every 10 seconds. The total average was calculated by taking the average of all the wind speeds. The running average was computed by taking the average of a given wind speed datum and all other wind speed data points that occurred before it. Unfortunately, Microsoft Excel could not compute more than one million averages, which also had averages in them. We devised a way to go about doing this through the following method:

$$R_1 = v_1 \tag{6}$$

$$R_i = R_{i-1}\frac{i-1}{i} + v_i\frac{1}{i}, for \ i = 2,3,\dots,total \ number \ of \ data \ points \tag{7}$$

Where R is the running average of a given wind speed and v is the wind speed. This method computes a given running average from the previous weighted average, thus eliminating any computational problems with Microsoft Excel.

5.4 Wind Turbine Test Rig Comparison to CFD Simulation

We wished to produce a graph similar to Figure 39 (from the CFD Flow Simulation section). Unlike Figure 39, this new graph is of the actual wind speed versus actual RPM, from the anemometer and test rig respectively, which can be seen in Figure 50:
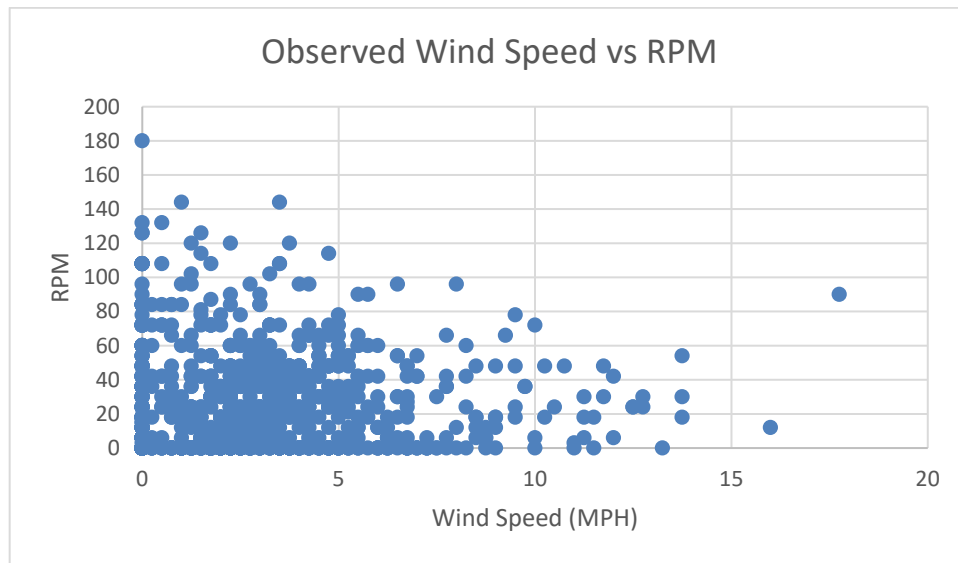
Figure 50 - Observed Wind Speed vs RPM

The data shows no correlation between the actual wind speed measured by the anemometer and the actual RPM of the wind turbine test rig. It was clear that it would be impossible to make any sort of comparison with the corresponding graphs of the CFD Flow Simulation data. Instead, we decided to focus our attention on why this graph had no trend.

5.5 Wind Turbine Test Rig Conclusion

A key piece of information that we found from our test rig and anemometer data was that the test rig takes time to spool up causing a delay in the RPM data when the wind speed spikes up or slows down. This can be seen in Figure 51, Figure 52, Figure 53, and Figure 54:
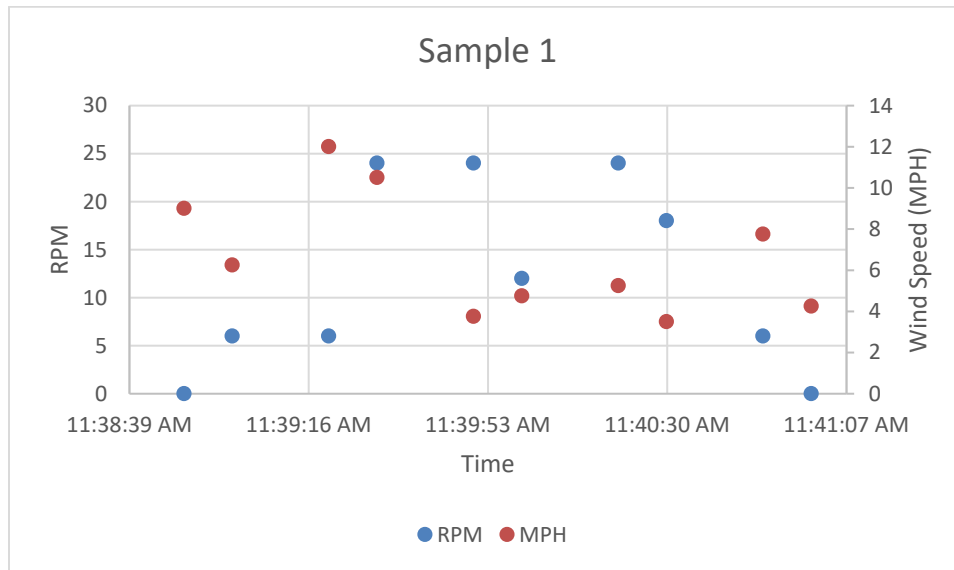
Figure 51 - Sample 1 of Wind Speed and RPM Data
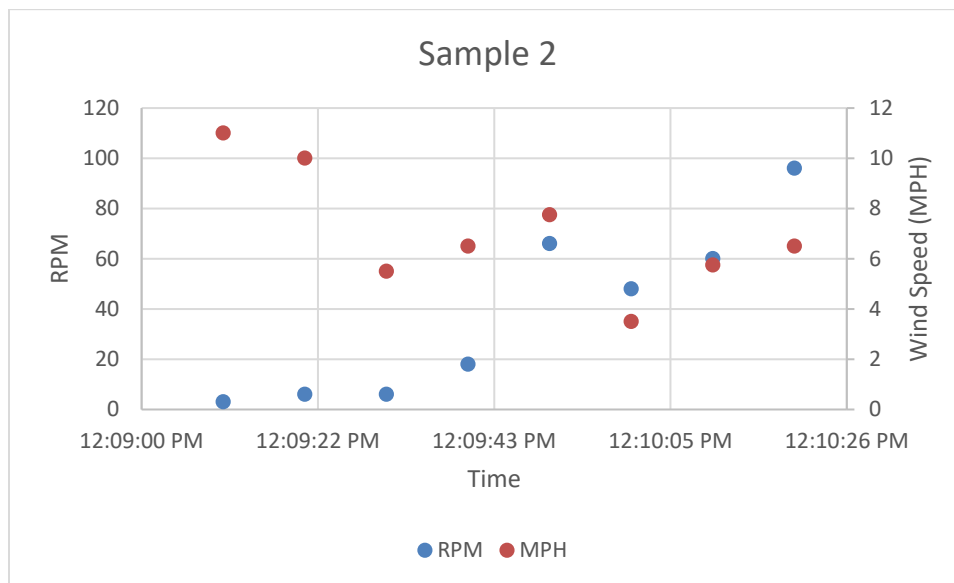
Figure 52 - Sample 2 of Wind Speed and RPM Data
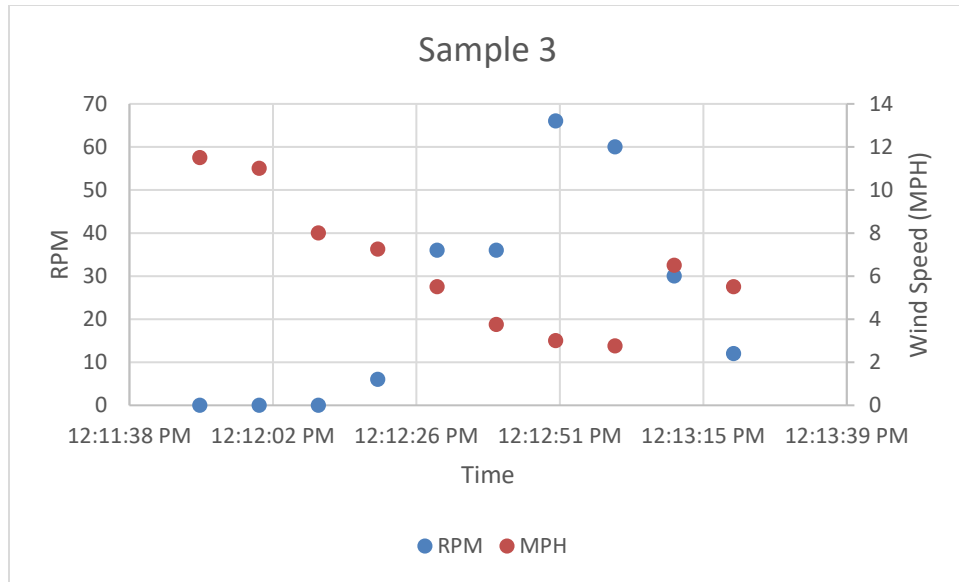
Figure 53 - Sample 3 of Wind Speed and RPM Data
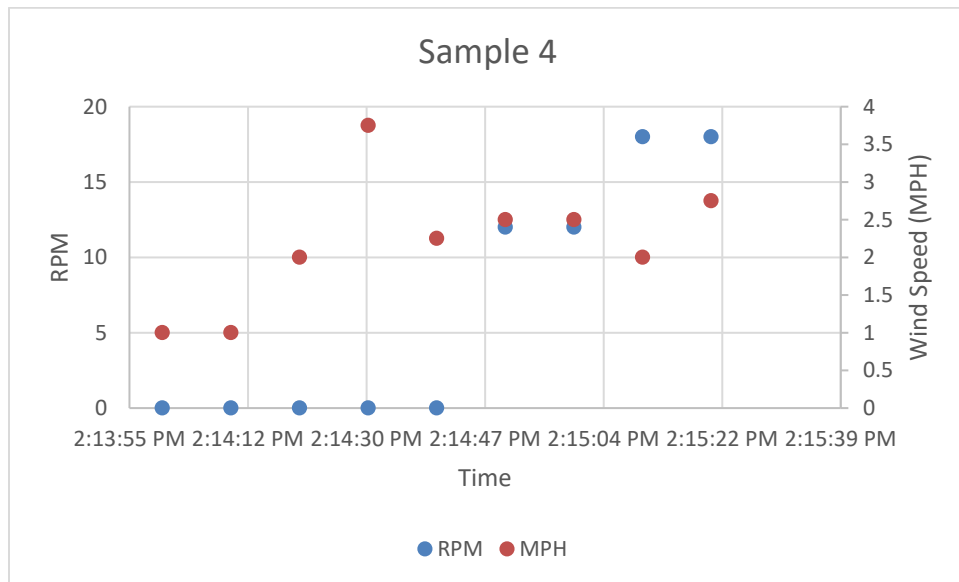
Figure 54 - Sample 4 of Wind Speed and RPM Data

These four samples show that there is a time delay between change in wind speed and change in RPM. This would explain why Figure 50 has no trend. We believe that this phenomenon is occurring due to the inertia of the wind turbine test rig. In order for the wind turbine test rig fan blades to increase their angular velocity, it will need to have the appropriate

70

angular acceleration to get it up to that angular velocity. This angular velocity takes time to overcome the inertia of the wind turbine test rig. In addition, the angular velocity will remain constant longer than the wind speed does. In essence, the angular velocity is "averaging out" when the wind speed spikes. This insight becomes important when revisiting the fact that the power in the wind is proportional to the cube of the wind speed. Large amounts of power are generated from these spikes in wind speed. However, because the angular velocity "evens out", much of that power is being used to overcome the inertia of the wind turbine. Therefore, we have ascertained that lighter wind turbines will be more efficient in extracting power from the wind than heavier wind turbines.

To underline this concept of power disparity, we took our 1.3 million data points occurring at 10-second intervals and calculated the power for each data point using 100% of the Betz limit. We then took the average of groupings of 6 consecutive data points to determine their average power in a minute. We repeated this process for 3-minute intervals and 5-minute intervals. Compared to the raw data of 10-second interval power outputs, the 1-minute average only yielded 80% of that power. The 3-minute average produced 71% and the 5-minute average produced 68%. This shows that the "averaging" effects of increased inertia decrease the efficiency of a wind turbine.

6.0 Future Considerations

For someone using our testing results to optimize their design of a wind turbine, it is necessary to explore topics related to electricity, wind, renewable energy, electric machines, existing residential wind turbines, and economics.

6.1 Electrical Concepts

First and foremost, the central aspects of electricity, namely current, voltage, and resistance, must be defined. Current is the rate at which charged particles passes through a certain point [9]. Direct Current (DC) is current that flows at a steady rate and in a single direction. Alternating Current (AC) is current that flows back and forth in a sinusoidal manner [9]. Voltage is the electrical potential energy difference across a circuit. Resistance is a material property that determines the potential difference given a certain amount of current flowing through it. Therefore, the following equation, known as Ohm's Law, determines resistance:

$$R = \frac{V}{I} \tag{8}$$

Where R is resistance, V is voltage, and I is current. A conductor that has a certain resistance is a resistor [9]. In an electrical device, power is the product of current and voltage, as shown below:

$$P = IV \tag{9}$$

Where P is power, I is current, and V is voltage.

Power loss through a resistor is converted into thermal energy, which is not useful for electrical applications, and can be denoted as:

$$P_{Loss} = I^2 R \qquad (10)$$

$$P_{Loss} = \frac{V^2}{R} \qquad (11)$$

Where R is the resistance of the wire, V is voltage, I is current, and P_{Loss} is power loss [9].

6.2 Renewable Energy

Approximately 10% of energy sources is renewable energy in the United States of America. Within this 10%, 23% make up wind-related energy sources. Other renewable energy sources include hydro (60%), biomass (13%), geothermal (4%), and solar (0.3%). However, these renewable energy sources are only about 33.3% efficient. The remaining 66.7% is lost to powering the plant itself, power losses in distribution lines, and thermal losses. Because renewable energy generators are designed so that they can only run under certain conditions (such as the wind blowing or the sun shining), they often get curtailed when the power supplied is greater than the demand. Nuclear reactors, on the other hand, will run almost all the time close to maximum power [9].

To incentivize the use of renewable energy, the United States government has created Renewable Energy Certificates (RECs). RECs are technology and environmental (non-energy) attributes that represent proof that 1 megawatt-hour (MWh) of electricity was generated from an eligible renewable energy resource, that can be sold separately from the underlying generic electricity with which they are associated. REC owners can retire them in exchange for financial compensation. In this sense, there is an incentive to use renewable energy such as wind power.

There are three ways to purchase RECs through: a Power Purchase Agreement, directly through a utility, and through an independent market [10].

Incentivizing renewable energy ultimately brings up the question of who will be willing to purchase it. We have identified an important, potential customer: wind turbine installation companies who could use our flow simulation and data collection to help them find potential locations to install wind turbines.

A second potential customer is the US military. In remote bases and posts in Afghanistan, the military uses gasoline generators to power their camps. However, it takes roughly two gallons of gasoline to transport one gallon of fuel. This means that the military uses about 70% of its gasoline consumption to transport the remaining 30% of gasoline [11]. To put this into monetary terms, the military must spend up to $400 to airdrop one gallon of gasoline [12]. A way to help reduce these high costs is to use wind power to produce electricity. Using our models, the US military could predict electrical output in new bases where known wind data is limited.

6.3 Wind Turbine Electric Machines

Wind turbines (and most other machinery that generates electricity) work in a way such that it is powered by a fluid in motion (in this case the wind) which passes through and spins the wind turbine blades, thus spinning the shaft. The generator then uses the energy from the rotating shaft to produce electricity [13]. The wind turbine's ability to produce electricity begins with Faraday's Law. Faraday's law is the derivative of magnetic flux with respect to time (the integral of a magnetic field over the area that it occupies), and this induces a voltage with a current in a closed conducting loop. Faraday's Law leads into the Hall effect. A Hall effect is when a

magnetic field perpendicular to a conductor strip that carries current produces voltage across the

conductor strip [9].

To generate power, you need an electric machine. A synchronous machine is one of the

three main types of electric machines. A synchronous machine has a grouping of conductors

known as an armature that is positioned in such a way that they can be moved through a

magnetic field and induce voltage. Typically, armatures are placed in stationary stators that are

close to a rotating magnetic field, which is either created through a permanent magnet or field

windings. Conductors receive DC current from the more popularly used field windings that can

either be spiraled around slow-spinning salient poles or found in faster moving rotating rotors.

The following equation shows how the speed of those rotors is determined by:

$$N(rpm) = \frac{120f}{p} \tag{12}$$

Where N is the rotor speed, f is the output frequency, and p is the number of poles [9]. In

general, three-phase synchronous machines convert mechanical torque to electrical power when

connected to the grid. Its rotor must spin at the same speed as other grid generators [13].

In addition to synchronous machines, there are also induction machines. Induction

machines do not operate at synchronous speed with a load. There are two types of induction

machines: wound rotor induction generators (WRIG) and squirrel cage induction generators

(SCIG) (made up of a copper/aluminum cage that is similar to one that is used for a pet squirrel).

A WRIG, which can operate at a controlled speed, supplies AC (with varying frequency) to the

rotor and the stator responds with 60 Hz of AC (frequency of the grid in the United States of

America). The frequency of the rotor always tries to maintain this 60 Hz by balancing out the

supplied AC frequency. If the rotor spins with a frequency of 65 Hz, the supplied AC frequency

responds with 5 Hz in the opposite direction. WRIGs require exciters, brushes, and slip rings. A

SCIG has its rotor shorted. The stator, as usual, is connected to the grid which has AC running

through it. This AC in the stator allows for the rotor to spin when torque is applied, thus

outputting AC voltage back into the grid at the same frequency it was inputted (60 Hz) [13].

6.4 Research on Existing Residential Wind Turbines

DC household wind turbines currently dominate the residential wind energy market.

From data of current DC household wind turbines on the market, we ascertained the efficiency,

as a percentage of 59.26% (The Betz Limit), for a 400-Watt wind turbine, 600-Watt wind

turbine, and 1500-Watt wind turbine. Figure 55, Figure 56, and Figure 57 below show power (in

Watts) versus wind speed (in MPH) provided by the manufacturer of the 400-Watt, 600-Watt,

and 1500-Watt wind turbines:
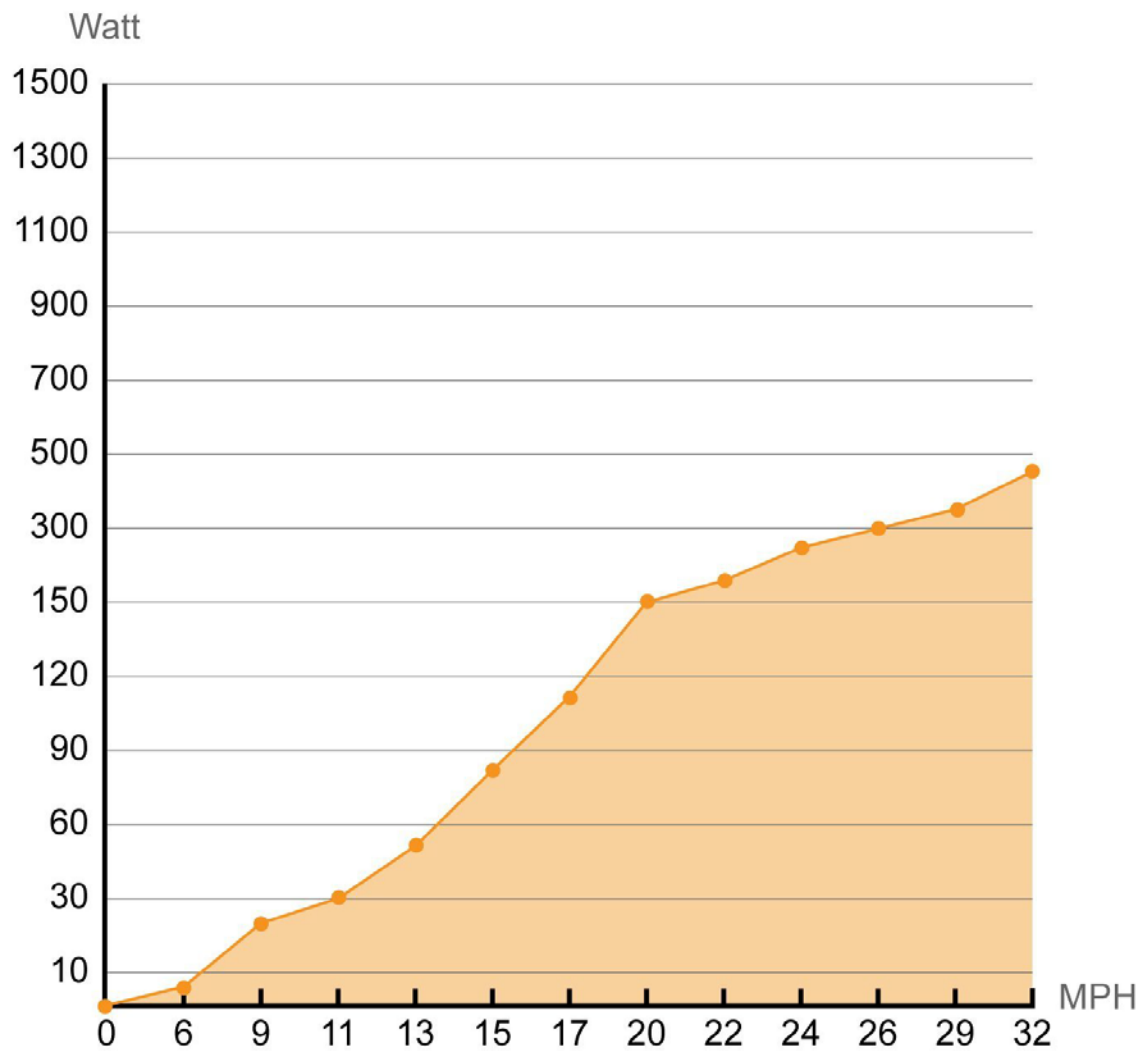
Figure 55 - 400-Watt DC Wind Turbine Power Output vs Wind Speed [14]
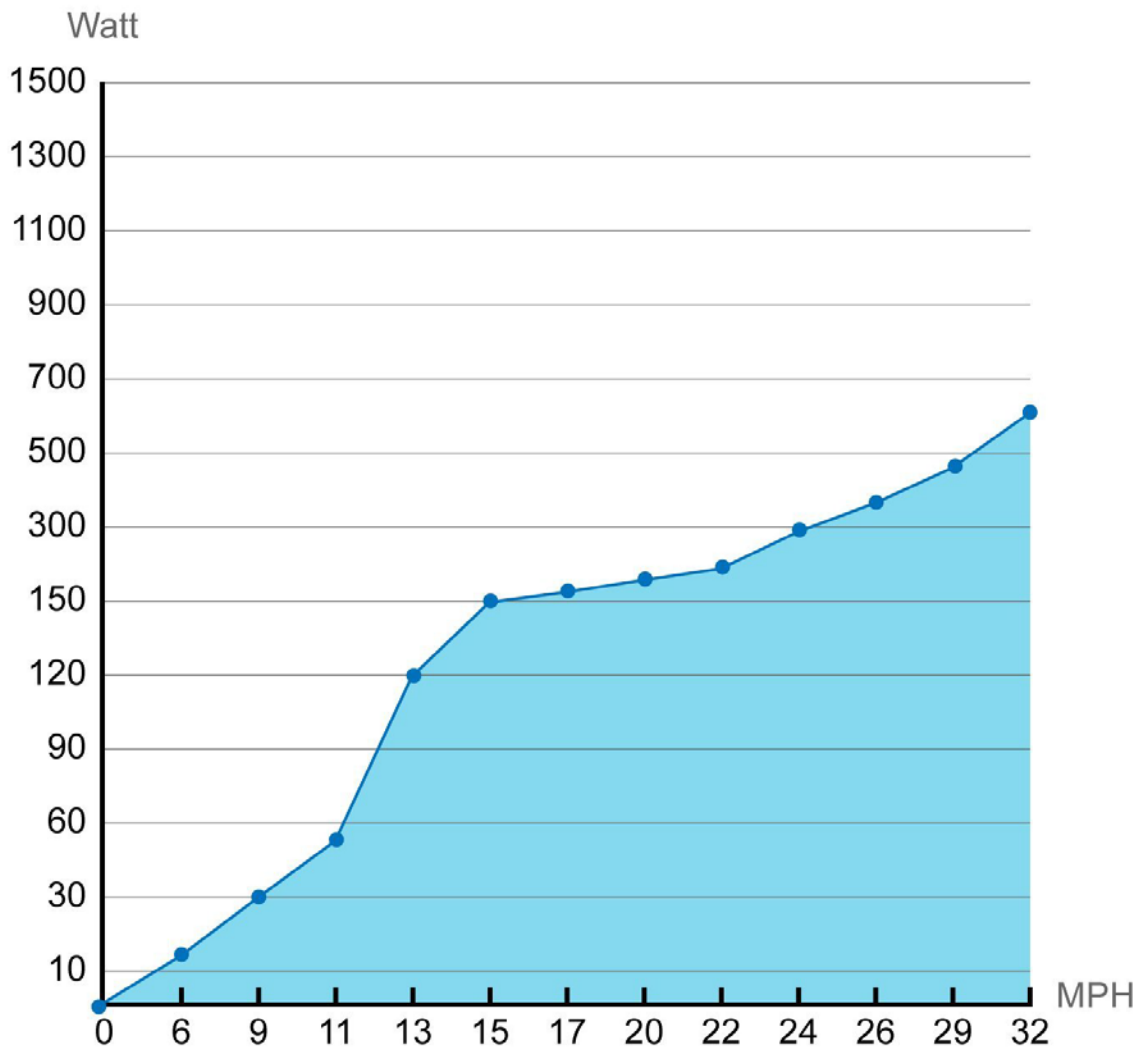
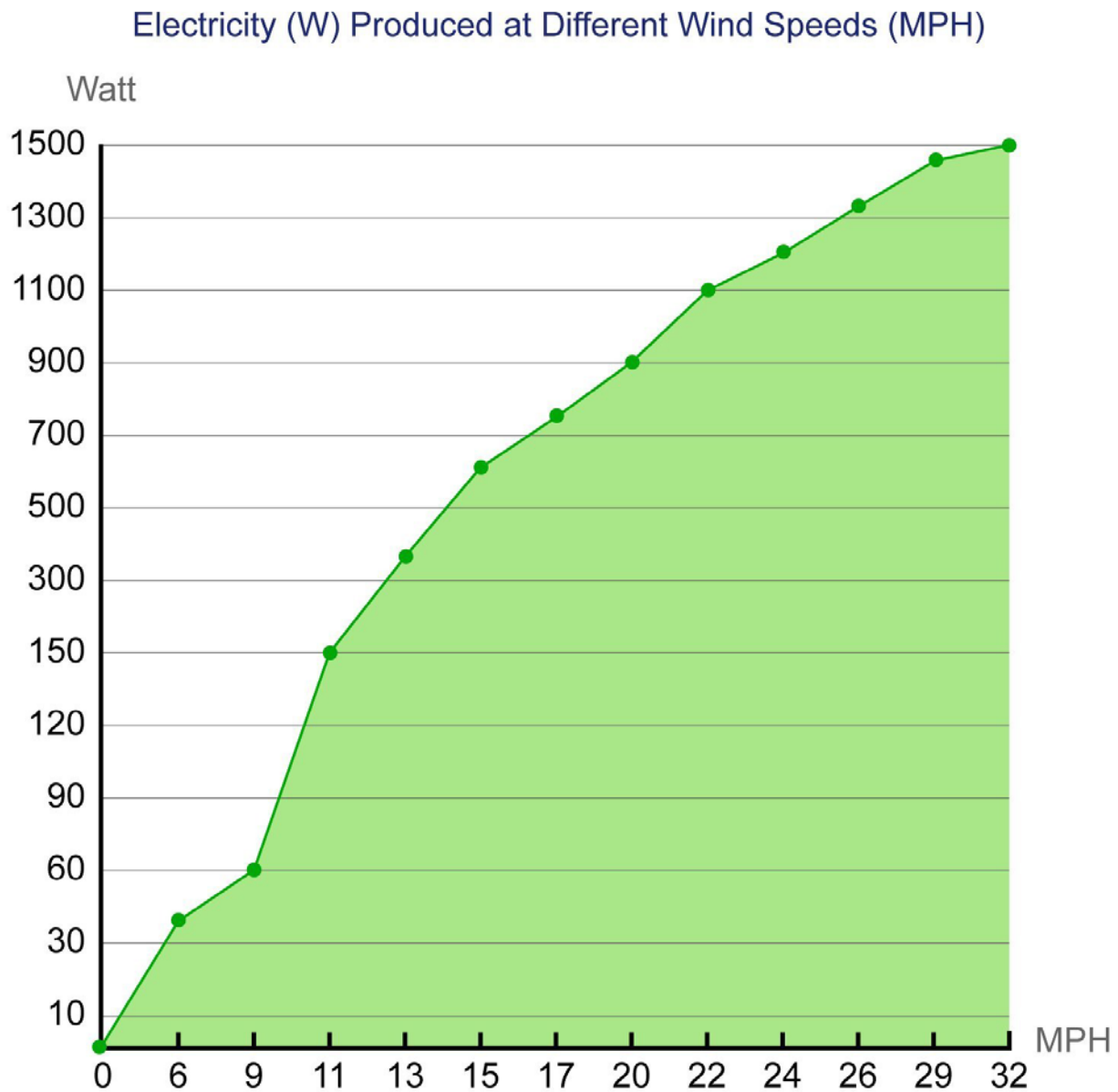*Figure 56 - 600-Watt DC Wind Turbine Power Output vs Wind Speed [15]*

Figure 57 - 1500-Watt DC Wind Turbine Power Output vs Wind Speed [16]

The manufacturers did not provide an efficiency for each turbine. We calculated the

efficiency of each wind turbine based on the data provided. We also conducted a trial-and-error

process to find the estimated curve that best matched the rated curve to ascertain each one's

efficiency. For each wind speed shown above, we calculated a power output with a theoretical

efficiency and blade area. We adjusted the efficiency until we achieved a minimum R^2 value for power output. Figure 58, Figure 59, and Figure 60 show the graphs related to this process:
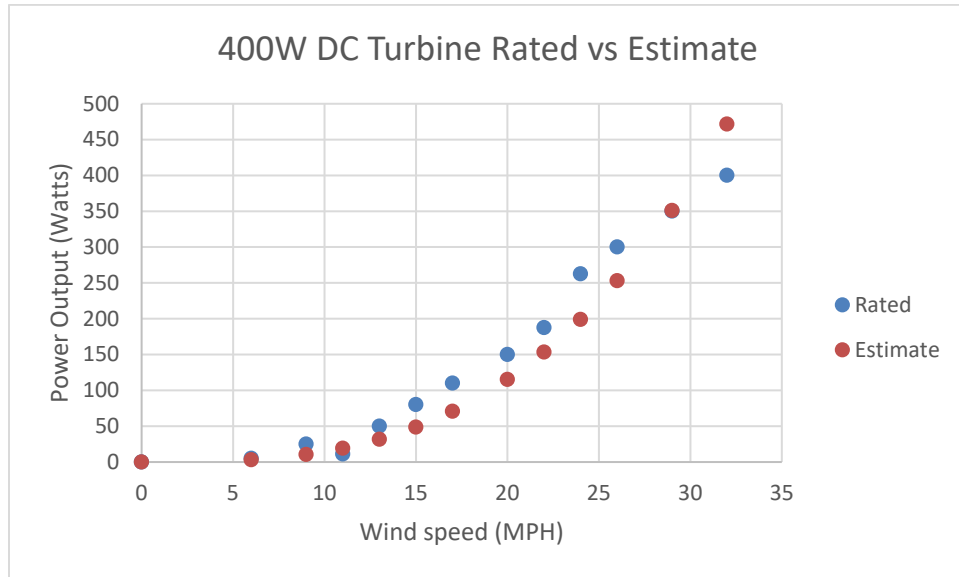

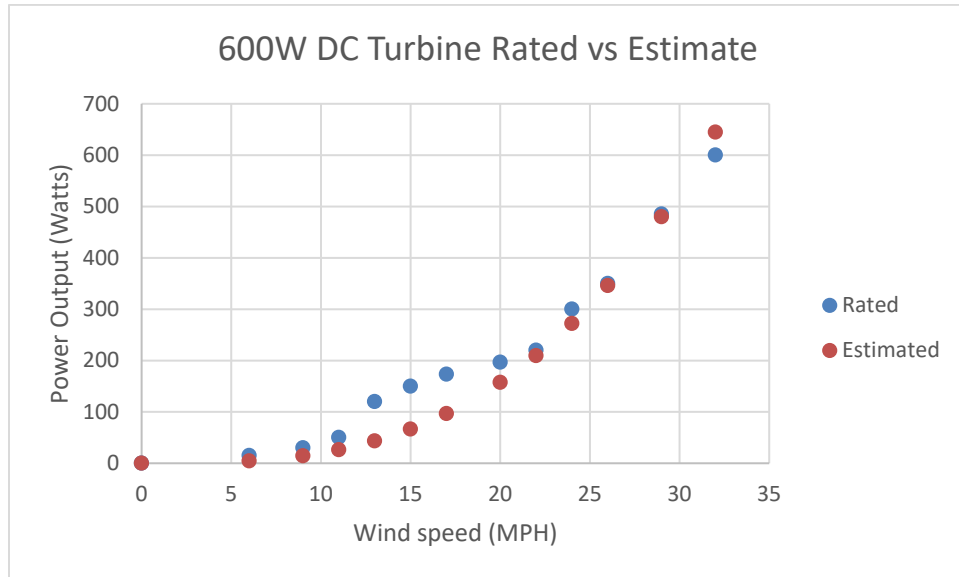*Figure 58 - 400W DC Turbine Rated vs Estimate*

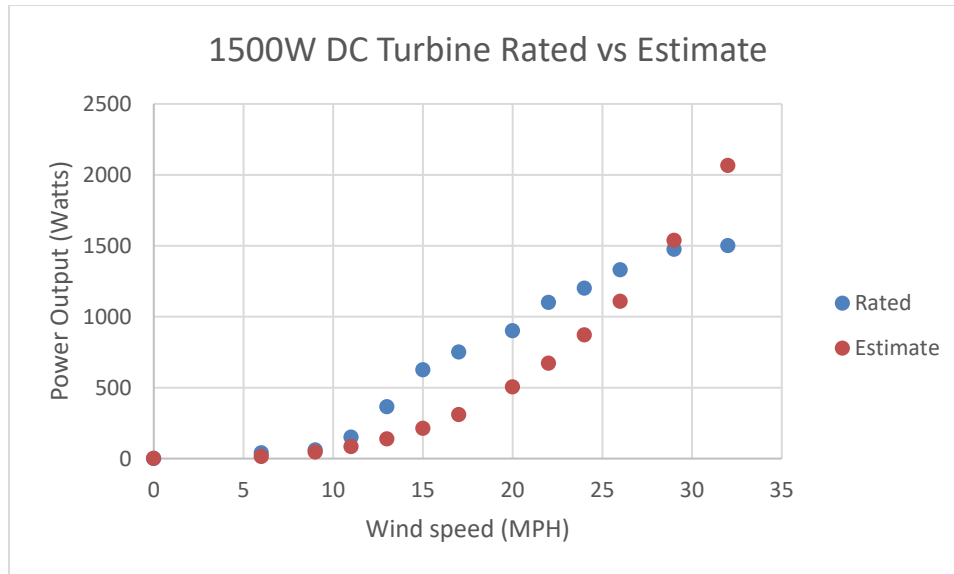*Figure 59 - 600W DC Turbine Rated vs Estimate*

Figure 60 - 1500W DC Turbine Rated vs Estimate

For the 400-Watt wind turbine, the efficiency is 38% of the maximum efficiency of 59.26%. For the 600-Watt wind turbine, the efficiency is 45% of the maximum efficiency. And for the 1500-Watt wind turbine, the efficiency is 85% of the maximum efficiency. This is data provided by the manufacturer, so these efficiencies may not be completely accurate. Ascertaining these efficiencies for new wind turbine prototypes can be made possible through the use of SolidWorks Flow Simulation, which is another reason why companies and organizations would value the work done for this MQP.

6.5 Present Value of Money

As with any venture, it is important to understand the finances of the undertaking. It is equally important to know that the value of money in the future is worth less today, which is known as inflation. This is due to the fact that money could be invested today and it could increase in value as a result. Given that nominal amounts of money throughout time do not necessarily have the same value, the present value can provide a form of standardization. This value can be obtained by the following equation:

$$P = \frac{F}{(1+i)^n} \qquad (13)$$

Where P is the present value, F is the future value, i is the interest rate, and n is the number of

years [9]. As of December 9, 2017, the interest rate is at 2.378% [17]. For the purposes of our

MQP, it is necessary for the wind turbine's investment interest rate to be greater in order to be a

successful venture. The cost of wind turbines is typical upfront. Their return on investment

usually occurs after a number of years, which is why the present value of money is important for

wind turbines.

References

[1] Masters, G. M., 2013, "Renewable and Efficient Electric Power Systems," .

[2] Anonymous "Sr001 Series 3 Amps to 150 Vdc Seperates," 2018(March 8,) .

[3] Anonymous "Pancake Slip Rings," 2018(March 8,) .

[4] Galliera, J., 2017, "Flow Simulation with Joe Galliera," .

[5] Colangelo, A., 2016, "Flow Simulation Basic Concepts," **2017**(September 6) .

[6] Galliera, J., 2017, "Parametric Versus Regular Study with Joe Galliera," .

[7] Anonymous "Inspeed Vortex Wind Speed Sensor," **2017**(September 8,) .

[8] Anonymous "Ambient Weather WS-0900-IP Wireless Internet Remote Monitoring Weather Station," **2017**(September 8,) .

[9] Halliday, D., Resnick, R., and Walker, J., 2014, "Fundamentals of Physics," Wiley, Hoboken, NJ [u.a.], .

[10] Meier, E., and Wallach, T., 2017, "Examining the Economic Viability of Clean and Renewable Electricity for WPI," Worcester Polytechnic Institute, Worcester Polytechnic Institute.

[11] Bakke, G., 2016, "The Grid: The Fraying Wires Between Americans and Our Energy Future," Bloomsbury USA, .

[12] Nathan Hodge, 2011, "World News -- U.S.'s Afghan Headache: $400-a-Gallon Gasoline --- Military Air Drops Fuel Barrels to Avoid Dangerous Convoys," Wall Street Journal, .

[13] Fitzgerald, A.E., Kingsley, C., and Umans, S.D., 2003, "Electric machinery," McGraw-Hill, Boston [u.a.], .

[14] Anonymous "400-Watt DC Wind Turbine Power Output Vs Wind Speed," .

[15] Anonymous "600-Watt DC Wind Turbine Power Output Vs Wind Speed," .

[16] Anonymous "1500-Watt DC Wind Turbine Power Output Vs Wind Speed," .

[17] Anonymous "Us 10-Yr (Us10y:U.s.)," **2017**(December 9,) .